

Contents lists available at ScienceDirect

Tissue and Cell

journal homepage: www.elsevier.com/locate/tice



The vicious cycle between nutrient deficiencies and antibiotic-induced nutrient depletion at the host cell-pathogen interface: Coenzyme Q10 and omega-6 as key molecular players

Darab Ghadimi ^{a,*}, Sophia Blömer ^b, Aysel Şahin Kaya ^c, Sandra Krüger ^d, Christoph Röcken ^d, Heiner Schäfer ^e, Jumpei Uchiyama ^f, Shigenobu Matsuzaki ^g, Wilhelm Bockelmann ^{a,1}

- ^a Department of Microbiology and Biotechnology, Max Rubner-Institut, Hermann-Weigmann-Str 1, Kiel D-24103, Germany
- ^b Faculty of Medicine, Christian-Albrechts-University of Kiel, Kiel 24105, Germany
- ^c Department of Nutrition and Dietetics, Faculty of Health Sciences, Antalya Bilim University, Antalya, Turkey
- d Institute of Pathology, Kiel University, University Hospital, Schleswig-Holstein, Arnold-Heller-Straße 3/14, Kiel D-24105, Germany
- ^e Laboratory of Molecular Gastroenterology & Hepatology, Christian-Albrechts-University & UKSH Campus Kiel, Kiel 24105, Germany
- f Department of Bacteriology, Graduate School of Medicine Dentistry and Pharmaceutical Sciences, Okayama University, Okayama, Japan
- g Department of Medical Laboratory Science, Faculty of Health Sciences, Kochi Gakuen University, Kochi, Japan

ARTICLE INFO

Keywords: Antibiotics Coenzyme Q10 Infection Inflammation Micronutrients Oxidative stress

ABSTRACT

The increasing prevalence of antibiotic resistance and pathological inflammation underscores the importance of understanding the underlying biochemical and immune processes that govern the host-pathogen interface. Nutrient deficiency, compounded by antibiotic-induced nutrient depletion, forms a vicious cycle of overt inflammation, contributing to bacterial toxin translocation in human inter-organ and intra-organs milieus. Coenzyme Q10 (CoQ10) and omega-6 linoleic acid (LA 18:2ω6) are integral to cellular membrane integrity and immune defense. However, the complex enzymatic steps at the host cell-pathogen interface remain poorly understood. This study is particularly timely, as it explores these knowledge gaps, which can inform the development of nutritional and therapeutic strategies that modulate or target these mechanisms. Using an infectiousinflamed cell co-culture model of the gut-liver axis, we exposed triple cell co-cultures of human intestinal epithelial cells (T84), macrophage-like THP-1 cells, and hepatic cells (Huh7) to linoleic acid-producing Lactobacillus casei (L. casei) and Pseudomonas aeruginosa strain PAO1 (PAO1). The cultures were incubated for 6 h in medium with or without ceftazidime antibiotic. PAO1 and L. casei exerted opposing effects on the secretion of Th1 cytokines IL-1β, IL-6, and the Th 2-type cytokine IL-10. Inoculation with PAO1 decreased CoQ10 and linoleic acid levels compared to uninfected controls. L. casei restored cellular health and biofunctionality impaired by PAO1, indicating its benefit to the host's well-being. The antibiotic ceftazidime exerted dual effects, alleviating PAO1 toxicity while marginally disrupting the beneficial effects of L. casei. Our results show how the vicious cycle of nutrient deficiency and antibiotic-induced nutrient loss reinforces pathological inflammation at the host cell-pathogen interface and highlights the need for more appropriate targeted antibiotic use that preserves essential nutrients like CoQ10 and omega-6 fatty acids. Inflammatory responses driven by opportunistic pathogens and LA-producing bacteria represent opposing immunometabolic pathways that may provide insights into novel approaches for treating infection and reducing antibiotic resistance.

1. Introduction

Nutrient deficiency and antibiotic-induced nutrient depletion can create a self-reinforcing cycle of inflammation that facilitates the translocation of bacterial toxic signal molecules within human interorgan and intra-organs. This interplay is particularly relevant on the gut-liver axis (Albillos et al., 2020), where host nutritional status, microbial activity, and immune responses converge. In this context,

^{*} Correspondence to: Department of Microbiology and Biotechnology, Max Rubner-Institute, Hermann-Weigmann-Straße 1, Kiel 24103, Germany *E-mail address*: darab.ghadimi@mri.bund.de (D. Ghadimi).

¹ Retired

understanding how key nutrients interact with antibiotic treatment and host-pathogen dynamics is essential for developing more targeted therapeutic strategies (Matthaiou et al., 2023; Jung et al., 2022; Shobha, 2019).

Coenzyme Q10 (CoQ10, ubiquinone) is a vitamin-like fat-soluble molecule located in cellular membranes and mitochondria, where it plays a crucial role in electron transport and antioxidant defense. Due to its bioenergetic and anti-inflammatory properties, CoQ10 is widely used in clinical nutrition, particularly in conditions characterized by oxidative stress and mitochondrial dysfunction (Burgardt et al., 2021; Fan et al., 2022).

Linoleic acid (LA, 18:2ω6), the parent compound of omega-6 polyunsaturated fatty acids (PUFAs), is an essential fatty acid that humans cannot synthesize de novo (Saini, Keum, 2018). It must be obtained from dietary sources or produced by the commensal gut microbiota such as Bifidobacterium and Lactobacillus (Peng et al., 2018). LA and its downstream metabolites participate in immune regulation, membrane architecture, and lipid signaling (Xu et al., 2025). In particular, both LA and CoO10 are integral components of cell membranes and participate in maintaining barrier integrity and immune homeostasis (Abi Nahed et al., 2025; Murea, LaLonde, 2017; Yang et al., 2020; Yip et al., 2023). Recent studies have shown that bacterial pathogens exploit host-derived lipids to support their growth and virulence. For example, Pseudomonas aeruginosa can hijack host fatty acids, including LA-derived arachidonic acid, to modulate host immune responses (Baker et al., 2018). Additionally, n-6 PUFAs, such as LA, have been shown to enhance the efficacy of certain antibiotics against pathogenic bacteria (Ham et al., 2025).

The pro-inflammatory label historically assigned to omega-6 fatty acids has been reevaluated in light of new evidence. While LA is a precursor of pro-inflammatory eicosanoids, clinical studies in healthy adults suggest that a higher intake of LA does not necessarily increase inflammatory markers. In fact, LA has been associated with anti-inflammatory effects and a reduction in cardiovascular risk and type 2 diabetes (Marklund et al., 2019; Xu et al., 2025). These findings underscore the dual role of omega-6 fatty acids in immune modulation, participating in both the initiation and resolution of inflammation (Brouwers et al., 2020; Innes, Calder, 2018; Kaviani et al., 2025; Lai et al., 2025; Marklund et al., 2019; Poli et al., 2023).

Antibiotic therapy, while essential in managing infections, can profoundly disrupt the gut microbiota, impair digestion, and alter host metabolism. By affecting microbial fermentation and protein digestibility, antibiotics can lead to macro- and micronutrient deficiencies (Felípez and Sentongo, 2009; Mantle and Golomb, 2025; Matthaiou et al., 2023; Patangia et al., 2022). Furthermore, antibiotics have been shown to exert direct effects on host cells, including mitochondrial dysfunction and shifts in host metabolomic profiles independent of microbial changes (Liu et al., 2025; Yang et al., 2017).

Despite increasing interest in the microbiota-nutrient-drug triad, little is known about how antibiotics influence the interaction between CoQ10 and omega-6 fatty acids at the host-pathogen interface. Emerging evidence suggests that CoQ10 and LA may form intermolecular interactions that facilitate membrane permeability and nutrient transport, possibly affecting drug delivery and immune response (Luo et al., 2025; Rehman et al., 2015; Tou et al., 2019). However, their combined behavior under antibiotic pressure in an inflamed or infected host milieu remains uncharacterized. Therefore, the main research gap is that no previous studies have explored the potential requirement for concomitant supplementation with CoQ10 and omega-6 LA during antibiotic exposure at the host-pathogen interface, particularly in the context of intestinal and liver crosstalk. The mechanistic basis by which antibiotics modulate this nutrient interaction in inflammatory conditions is still poorly understood. To address this gap, we used a triple cell co-culture model consisting of intestinal epithelial cells, macrophages, and hepatocytes, cell types that collectively represent the gut-liver axis (Albillos et al., 2020; Hsu and Schnabl, 2023). This model allows us to simulate physiological interactions between the intestinal barrier, immune response, and hepatic metabolism during infection and antibiotic treatment. Within this model, intestinal epithelial cells serve as the first barrier against pathogens and are essential for nutrient absorption and mucosal immunity (Didriksen et al., 2024). Macrophages are key players in innate immunity, orchestrating inflammatory responses, and maintaining tissue homeostasis (Muller et al., 2020; Nakagaki et al., 2018). Hepatocytes, the principal functional cells of the liver, regulate systemic metabolism, detoxify xenobiotics, and respond directly to microbial signals (Etienne-Mesmin et al., 2016; Schulze et al., 2019). The interconnectedness of these cells is vital to understanding the dysfunction of the gut-liver axis during infection. Moreover, different cell types exhibit unique capacities to metabolize LA and respond to CoQ10, making this model ideal for examining nutrient-antibiotic interactions at multiple levels. Accordingly, we hypothesized that nutrient deficiency and antibiotic-induced nutrient depletion promote a vicious cycle of pathological inflammation, mediated by Th1/Th2 cytokine signaling between intestinal cells and hepatocytes. This cycle facilitates the translocation of toxic bacterial signals and exacerbates inflammation at the host-pathogen interface. Furthermore, we hypothesized that co-supplementation of CoQ10 and LA could mitigate these effects. To test this, we investigated the impact of ceftazidime, a broad-spectrum antibiotic, on nutrient signaling and inflammation within this in vitro infectious-inflamed model, both in the presence and absence of CoQ10 and omega-6 supplementation. This study distinguishes itself from the excellent previously cited studies, which have focused primarily on the effects of antibiotics on bacterial resistance or host nutrient absorption in vivo. In contrast, we employ an in vitro infectious-inflamed triple cell co-culture model to directly investigate the interplay between pathological inflammation (rather than physiological inflammation), nutrient-linked biomarkers (e.g., CoQ10 and omega-6), and Th1/Th2 cytokine responses. This control system enables a mechanistic evaluation of the complex triad formed by antibiotics, nutrients, and host-pathogen interactions in modulating host cell metabolism and immune signaling, an area that has remained largely unexplored in previous studies. By bridging the microbial, immunological, and nutritional axes, this study provides an integrative perspective that is not typically revealed in previous studies. Furthermore, this study provides new insights into pathophysiology nutrition dysregulation associated with inappropriate antibiotic use and highlights the nutritional and therapeutic potential of nutrient-based interventions in preserving host defense mechanisms. Illustrative figures accompanying this work visually summarize key molecular pathways and interactions, reducing the need for extensive textual descriptions and enhancing clarity for the reader.

2. Materials and methods

2.1. Reagents and kits

Advanced DMEM (Gibco, Cat. #12491015), disposable & sterile mini cell scrapers (Cat. #NC0325221, designed for even use in 96-wells), Dulbecco's Phosphate Buffered Saline (DPBS, Gibco, Cat. #14190250), Fetal Bovine Serum (FBS, Gibco, Cat. #A5670701), and Transwell inserts (0.4-µm pore size, 24-mm diameter) in Transwell cultures (Corning, Cat. #3450) were purchased from Fisher Scientific GmbH (Schwerte, Germany). Human IL-1 β (Cat. #900-K95), IL-6 (Cat. #900-K16), IL-10, and TNF- α ELISA kits were purchased from PeproTech (Hamburg, Germany). The Human Coenzyme Q10 ELISA kit (Cat. #ABIN6975185) was purchased from antibodies-online GmbH (Aachen, Germany). Ceftazidime (Cat. #CDS020667) and phorbol-12-myristate-13-acetate (PMA, Sigma Cat. #P8931) were obtained from Sigma Chemical (Sigma-Aldrich, Taufkirchen, Germany).

2.2. Literature search

To support the development of the triple in vitro cell co-culture model

and the experimental design and to confirm the selection of bacterial strains and antibiotic treatments, a targeted literature search was performed using PubMed, Ebsco, Google Scholar, and Science Direct. The search strategy incorporated the primary keywords of this study, including antibiotic-induced inflammation, antibiotic-induced dysbiosis, gut–liver axis, intestinal immune hepatic cell co-culture, bacteria translocation, in vitro host–microbe interactions, metaflammation, infection, and cytokine. Relevant studies were reviewed to identify experimental conditions, co-culture systems, and microbiota models. We excluded letters to the editor, historic reviews, and unpublished data from the analysis. No specific date restrictions were applied.

2.3. Bacterial strains and growth conditions

The Gram-positive *Lactobacillus casei* strain (*L. casei*, ATCC 334) and the Gram-negative *Pseudomonas aeruginosa strain* PAO1 (PAO1, DSM 22644) were used as a natural linoleic acid producing bacterium (Peng et al., 2018) and an opportunistic pathogen model bacterium (Wood et al., 2023), respectively.

Among gram-negative opportunistic human pathogens, the risk of *P. aeruginosa* as a foodborne pathogen in the gut can be summarized as follows: Recent studies have reported a remarkable rise in foodborne contamination by multidrug-resistant (MDR) *Pseudomonas aeruginosa*, whose global spread poses a serious threat to public health. *P. aeruginosa* causes substantial tissue damage and is highly resistant to antibiotics, leading to potentially fatal infections in both humans and animals. This pathogen has been detected in various food groups and is particularly difficult to treat due to its rapid proliferation, ability to form biofilms, and possession of both intrinsic and acquired antimicrobial resistance genes (ARGs) commonly carried by this species. Furthermore, antibiotic-induced disruption of the intestinal microbiota (dysbiosis) facilitates colonization of the gut by MDR *P. aeruginosa*. Its rapid emergence and dissemination continue to jeopardize public health and food safety (Li et al., 2023; Ramsay et al., 2023).

The culture method of PAO1 and the rationale for its use in this study have previously been described in detail (Ghadimi et al., 2023; Li et al., 2023; Ramsay et al., 2023; Uchiyama et al., 2016). For routine maintenance and enumeration of PAO1 bacterial culture, bacterial counts (colony-forming units per milliliter, CFU/ml) were obtained by serially diluting the strain in 0.09 % B. Braun isotonic saline solution, plating on Luria-Bertani (LB) agar, and incubating at 37 $^{\circ}\text{C}$ for 48 h before quantifying the colonies. To prepare an active and synchronized bacterial suspension required for three independent experiments and to ensure viability before co-culture with eukaryotic host cells, bacterial colonies of PAO1 were stored at 4 °C. Before each experiment, a single colony was inoculated into a test tube containing 5 ml of LB broth and grown overnight at 37 °C with gentle shaking at 120 rounds per minute (rpm). The bacteria were then collected by centrifugation (4000 rpm, 5 min, 4 °C), washed twice in Dulbecco's phosphate-buffered saline (DPBS) and resuspended in fresh DPBS. The suspension was then adjusted (diluted) to an optical density (OD) of 0.2 at 600 nm, measured using a 1000 µl Eppendorf Vis Cuvette in an EPPENDORF biophotometer. This corresponded to an approximate bacterial concentration of 2×10^9 CFU/ml and was referred to as the original bacterial culture. The original bacterial cultures were mixed by vertexing, and then $50 \mu l$ of the bacterial suspension was added to the inside of the designated inserts with T84 monolayer cells (as described in the section 'Inflamed co-culture model').

Lactobacillus casei ATCC-334 (L. casei), a natural bacterial model known to produce linoleic acids (Peng et al., 2018), was obtained from the American Type Culture Collection (ATCC, LGC Standards GmbH, Wesel, Germany). For routine maintenance, L. casei cultures were kept on agar slopes and grown at 37 °C in MRS broth. For bacterial enumeration, overnight cultures were grown anaerobically at 37 °C using an anaerobic workstation (A45; Don Whitley Scientific, Bingley, UK). After growth, colony-forming units (CFU) were determined by

performing serial dilutions in MRS broth and plating onto agar plates. Plates were then incubated under anaerobic conditions for 48 h before colony counting. The preparation of *L. casei* for co-culture with eukaryotic host cells was followed by the same protocol as *P. aeruginosa* PAO1, except that *L. casei* was grown under anaerobic conditions. A bacterial-to-host cell ratio of 1.7:1(CFU to host T84 cells) was used for both *L. casei* and PAO1 in duplicate inserts, as described in the section 'Inflamed co-culture model'). This ratio was chosen because the bacteria-to-cell ratio in the human body is estimated to be approximately 1:1–1.618 (Murali and Alka, 2024; Sender et al., 2016).

2.4. Cell culture maintenance

The human intestinal epithelial T84 cell line was obtained from the American Type Culture Collection (ATCC CCL-248, LGC Standards GmbH, Wesel, Germany). Cells (passage numbers 19–23) were cultured in T-75 cell culture flasks using Advanced Dulbecco's Modified Eagle Medium (Advanced DMEM) supplemented with 5 % (v/v) fetal bovine serum. For polarized monolayer formation, cells were seeded (in appropriate sets of duplicate inserts) at a density of 2.4×10^5 cells per well onto Transwell inserts (0.4- μ m pore size, 24 mm diameter; Corning, Cat. #3450) and cultured for 7–8 days. The culture medium was changed twice weekly, with 1.5 ml added to the upper chamber and 2.6 ml to the lower chamber.

The formation of tight junctions was functionally assessed by measuring transepithelial electrical resistance (TEER) across the monolayers using an epithelial volt-ohmmeter (Millicell ERS-2, Merck Millipore, Darmstadt, Germany), according to the manufacturer's instructions. The electrical resistance of the uninfected monolayers ranged from 600 to 700 $\Omega \times \text{cm}^2$ after subtracting the resistance of a cell-free filter. Growth curves were determined by dissociating cells from the Transwell inserts using TrypLE Express Enzyme (Gibco, Cat. #12604013), followed by manual cell counting using a Neubauer counting chamber. Based on morphological and biochemical features, as well as functional responses to microbial products such as butyrate and LPS, T84 monolayers are considered superior to Caco-2 cells as a model of human colonocytes (Devriese et al., 2017). Only T84 monolayers with a TEER of \geq 700 $\Omega \times \text{cm}^2$ were used in the experiments; monolayers with TEER values below this threshold were excluded from further processing.

Huh7 human liver cells (from our frozen cells stock stored in liquid nitrogen) were from the Japanese Collection of Research Biosource Cell Bank (JCRB0403 HuH-7; FUJIFILM Wako Chemicals Europe GmbH, Neuss, Germany). Cells were maintained in standard DMEM medium supplemented with 5 % FBS and 1 % non-essential amino acids, as previously described in detail (Ghadimi et al., 2024). Cells were routinely split at ~ 80 % confluence and used for experiments at passages 18–24 after thawing.

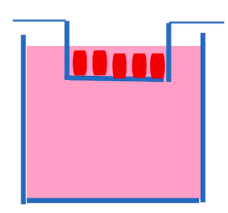
The culture medium for both epithelial and hepatic cell lines was refreshed every 2–3 days. Once the cells reached 80–90 %confluence, they were washed with DPBS and treated with TrypLE Express Enzyme for 5 min at 37 $^{\circ}$ C. The enzymatic reaction was then neutralized by adding complete medium, after which the cells were centrifuged and split into new cell culture flasks for passaging.

The THP-1 cell line (ATCC: TIB-202) was also obtained from the ATCC and cultured in T-75 cell culture flasks as a suspension (passage numbers 14–22). Once the cells reached confluence and the appropriate density, they were centrifuged and divided into new cell culture flasks. For differentiation, THP-1 cells were harvested, centrifugated, resuspended, maintained, and treated with phorbol myristate acetate (PMA, 25 ng/ml) to induce differentiation into macrophage-like cells. The differentiated THP-1 macrophages were then seeded on the underside of inverted Transwell inserts, as previously described in detail (Ghadimi et al., 2024; Calatayud et al., 2019; Klein et al., 2013).

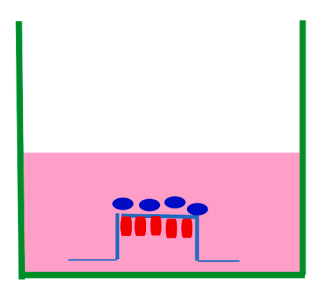
All cell lines were cultured in a humidified incubator at 37 °C with 5 % CO₂ using a Thermo Scientific Heracell 150i incubator equipped

with variable oxygen control. All cell lines were tested for Mycoplasma contamination using the MycoStrip Mycoplasma Detection Kit (InvivoGen, Toulouse, France), following the manufacturer's instructions. The endotoxin-free status of all cell cultures was assessed using the LAL Gel Clot Assay (Pyrogent TM Plus, Cat. #N294-03, Lonza, Cologne, Germany) with a detection sensitivity of 0.3 endotoxin units (EU).

For infection experiments, cells were used once they reached >90~% confluency.



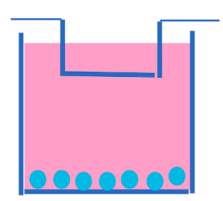
On day 0, T84 cells at confluent status were seeded onto the inside of the insert above the membrane.



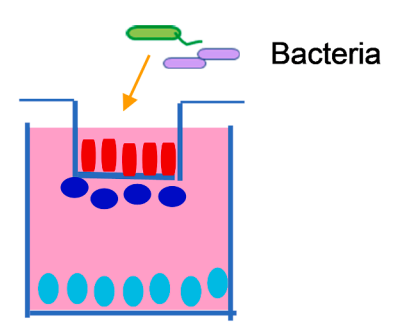
On day 8, the transwell insert containing T84 cells was inverted on a petri dish (100 mm x 50 mm H). THP-1 cells were afterward seeded (5.0 x 10⁴ cells/Transwell) on the underside of the Transwell membrane and incubated for 2 h to allow the cell adhesion. The transwell membrane was inverted again and placed on the well.

2.5. Triple cell co-culture

Triple cell co-cultures were prepared as previously described (Ghadimi et al., 2024), and the four-stage setup is shown schematically in Fig. 1. Day 0: T84 cells at confluent status were seeded inside Transwell inserts on the upper surface of the membrane (as described above). Day 6: Huh7 cells $(1.5 \times 10^6 \text{ per well})$ at confluence were seeded in separate six-well plates suitable for Transwell inserts, 72 h before T84 polarization was completed. Day 8: Transwell inserts containing



On day 6, Huh7 cells at confluent status were seeded in separate transwell-suitable six-well plates 72 h before T84 polarization ended.



Assembling triple co-culture:

T84/THP-1 co-cultures pre-grown for 8 days were placed directly on top of the Huh7 cells in the transwell-suitable six-well plates.

Fig. 1. Schematic representation of the triple co-culture model simulating the human gut–liver axis under infectious-inflamed milieu. The system integrates three human cell types: intestinal epithelial T84 cells (barrier), macrophage-like THP-1 cells (immune), and hepatocyte-derived Huh7 cells (metabolic). On Day 0, confluent T84 cells were seeded on the upper surface of a Transwell insert. On Day 6, confluent Huh7 cells were seeded in separate Transwell-compatible 6-well plates. On Day 8, the T84-containing insert was inverted (within a 100 mm×50 mm H petri dish), and THP-1 cells were seeded on the underside of the membrane and allowed to adhere for 6 h. The insert was then returned to its upright position and placed over Huh7 cells to assemble the triple co-culture. Pathogenic bacteria (*P. aeruginosa* PAO1) were added to the apical side (inside the insert), allowing selective infection of T84 cells while THP-1 and Huh7 cells remained unexposed. This setup allows the investigation of nutrient-pathogen-antibiotic interactions across epithelial, immune, and hepatic compartments.

polarized T84 cells were inverted onto a 100 mm imes 50 mm H-style Petri dish. This deep dissection dish is well suitable for handling larger specimens or inserts that must be fully submerged in medium for proper cell seeding and handling. Macrophage-like THP-1 cells (0.8 \times 10 6 cells per insert) were then seeded on the underside of the inverted Transwell membrane and incubated for 6 h to allow adhesion. Afterward, the inserts were again returned to their original orientation and placed in the well. To complete the triple co-culture assembly, the T84/THP-1 co-cultures (pre-grown for 8 days) were placed directly over the Huh7 monolayers in the six-well Transwell-suitable plates. The appropriate number of assembled triple co-cultures was adjusted according to experimental group requirements and was subsequently used in the inflamed co-culture model described in the next section. To calculate the number of bacterial cells added (at the beginning of the experiment) per insert, two additional separate Transwell inserts were included solely for cell counting prior to bacterial inoculation. These cell counts were used to calculate the bacteria-to-cell ratio (1.7:1) at the start of the inoculation experiments.

2.6. Inflamed co-culture model

As a preliminary quality control step, the co-cultured T84, THP-1, and Huh7 cells were inspected under an inverted microscope to ensure the absence of contamination. To simulate an infection-associated inflammatory milieu, *P. aeruginosa* (PAO1) was used, as it induces acute inflammatory responses similar to those that occur in vivo (Wood et al., 2023).

Before inoculating the triple cell co-cultures, the T84 cells of two separate inserts (as indicated above) were first counted to determine cell concentration and subsequently calculate the bacteria-to-cell ratio. Then, to ensure bacterial viability and accurately quantify the number of bacterial cells added at the start of the experiment, a direct microscopic count was performed using a Petroff-Hausser counting chamber with methylene blue staining. For this, 50 µl of the original overnight bacterial culture suspension (prepared as described in Section 2.3) was added to the apical side of the desired inserts containing T84 monolayers. Bacteria were added to T84 cells with a multiplicity of infection (MOI) of 1.7: 1. This ratio approximates the bacteria-to-human cell ratio in the human body, which ranges between 1:1 and 1.618 (Murali and Alka, 2024; Sender et al., 2016). The assembled triple co-cultures were divided into four experimental groups: (1) uninfected control cells, (2) P. aeruginosa (PAO1), (3) Lactobacillus casei (L. casei), and (4) P. aeruginosa + L. casei. Cells were then incubated for 6 h in standard culture medium or in medium supplemented with 1 mg/ml ceftazidime, a clinically relevant antibiotic used to treat a wide range of P. aeruginosa infections (Ramsay et al., 2023). Control co-cultured cells received only culture media. The apical compartments (upper) were filled with 1.5 ml of cell culture medium and the basolateral compartments (lower) with 2.6 ml (final volume). Subsequently, 10 µl of apical medium was taken and mounted on a Petroff-Hausser Bacteria Counter Chamber (calibrated slide, Cat. #3900) and the numbers of bacterial cells were determined under a light microscope. All cultures were then incubated in a humidified incubator at 37 °C, with 5 % CO2 and 3 % oxygen (physioxia conditions), using a Thermo Scientific Heracell 150i incubator with variable oxygen control. Each experiment was tested in at least two replicates and the experiments were independently repeated a minimum of three times to ensure the validity of the results. After the 6-hour incubation period was completed, the following procedures were carried out sequentially. First, 10 µl of apical medium was taken and mounted on a Petroff-Hausser Bacteria Counter Chamber to determine the number of bacterial cells under a light microscope. The percentage of bacterial growth or reduction was calculated by subtracting the number of bacteria remaining after 6 h from the initial number of bacteria added to the insert, dividing by the initial number of bacteria and then multiplying by 100. The media was then aspirated, centrifuged to remove cells and debris, sterilized using a 0.2 µm filter, and the

supernatant was stored at $-80\,^{\circ}\text{C}$ for future use. Subsequently, to assess the integrity and function of T84 cell monolayers, changes in monolayer permeability were evaluated by measuring TEER, as described above. Background resistance was determined using an empty culture insert. The TEER of the insert with medium alone was subtracted from the measured TEER, and the final resistance was calculated in ohms multiplied by the insert area in square centimeters ($\Omega \times \text{cm}^2$).

Second, T84, THP-1, and Huh7 cells were washed twice in DPBS and carefully scraped separately from cell culture inserts and wells using disposable sterile mini cell scrapers. The cells were then transferred to separate 15 ml or 50 ml tubes and centrifuged for 5 min at room temperature. After centrifugation, the supernatant was removed, and the resulting cell pellets were resuspended in pre-warmed cell culture medium. Next, a small sample volume (approximately 10 µl) of the pooled cell suspensions (from duplicate wells) was mixed with 10 μ l of 0.4 %trypan blue dye before cell counting. Subsequently, 10 µl of this mixture was loaded into an improved Neubauer counting chamber (Millicell Disposable Hemocytometer, MDH-4N1, Merck Darmstadt, Germany). The numbers of viable and non-viable cells were determined using the hemocytometer, and cell viability was calculated as the percentage of viable cells out of the total number of cells counted. The remaining cell suspensions were divided into three portions and further processed for the simultaneous determination of total CoQ10 content, total omega-6 levels, and alkaline phosphatase activity assays, as described in the following sections.

2.7. Total omega-6 fatty acid profile of co-cultured cells.

To determine total omega-6 fatty acids derived from linoleic acid (LA; $18:2\omega6$) and CoQ10, a portion (Portion I) of the pooled cell samples from duplicate wells (prepared as described above) was used to analyze the total content of cellular omega-6 fatty acids. The analysis was performed using a human omega-6 fatty acid ELISA kit (Cat. #FAomega6 MBS756363; MyBioSource), following the manufacturer's instructions. The samples were tested in triplicate, and a standard curve was generated and used to extrapolate omega-6 fatty acid concentrations in the samples.

2.8. Determination of total cellular CoQ10

Total cellular CoQ10 was extracted using a separate portion (Portion II) of each pooled cell sample. Quantification of CoQ10 levels was performed using a Human Coenzyme Q10 ELISA Kit (Cat. #MBS165643; MyBioSource), following the manufacturer's instructions. The samples were analyzed in duplicate. Optical density (OD) measurements were taken at 450 nm using a microplate reader (Tecan). A standard curve was generated and used to extrapolate the CoQ10 concentrations in the samples.

2.9. Measurement of Th1 and Th2-type cytokine protein secretion

The secretion levels of Th1-type cytokines (IL-1 β , IL-6) and Th2-type cytokine (IL-10) in cultured supernatants were measured using commercially available enzyme-linked immunosorbent assay (ELISA) kits (BD Bioscinces or PeproTech GmbH), according to the manufacturer's instructions.

2.10. Alkaline phosphatase activity assay in cell lysates

Portion III of the pooled cell suspensions was processed to determine alkaline phosphatase activity (ALP) in cell lysate supernatants. The assay was performed at 37 $^{\circ}$ C using p-nitrophenyl phosphate (pNPP) as a substrate, with a commercial ALP assay kit (Cat. #MAK447; Sigma-Aldrich, Taufkirchen, Germany), following the manufacturer's protocol. Briefly, cells were washed with DPBS and lysed by adding lysis buffer containing 10 mM Tris-HCl (pH 8.0), 1 mM MgCl₂, and 0.5 %

Triton X-100. The lysates were centrifuged at 10,000 rpm for 5 min at 4 °C. The supernatant was collected and 25 μ l aliquots were used in triplicate for the ALP activity assay. The absorbance (optical density) of *p*-nitrophenol, the reaction product, was measured at 405 nm using a GENios Tecan microplate reader. ALP activity was expressed as the mean units per milliliter(U/ml) of the sample \pm standard error of the mean (SEM).

2.11. Analysis of metabolic markers of cell lysate and culture supernatant

T84, THP-1, and Huh7 cells were co-cultured in 6-well Transwell inserts and treated as described above (outlined in the 'Inflamed Co-Culture Model' section). After 6 h of incubation, the supernatants of the co-cultured cells were collected and stored at $-80\,^{\circ}$ C. The cells were then washed twice with DPBS and collected separately using sterile disposable mini cell scrapers. The pooled cells from duplicate wells and inserts were then lysed by adding lysis buffer containing 10 mM Tris-HCl (pH 8.0), 1 mM MgCl₂, and 0.5 % Triton X-100. After centrifugation $(3000 \times g, 15 \text{ min})$, the cell lysate supernatants were collected for intracellular analysis of high-density lipoprotein cholesterol (HDL-C) and triglycerides. The levels of glucose, iron, HDL-C, and triglycerides in both cell lysates and culture supernatants were determined enzymatically using commercially available assay kits, following the manufacturer's instructions (Thermo Fisher Scientific; Cat. #981823 for HDL-C, Cat. #981236 for iron, and Cat. #981301 for triglycerides). Measurements were taken photometrically at 546 nm using a Konelab 20i biochemistry analyzer (Thermo Fisher Scientific, Darmstadt, Germany) following the standard procedure, with the exception that 20 µl of supernatants were used instead of serum.

2.12. Competitive exclusion assay

A competitive exclusion assay was conducted as previously described (Ghadimi et al., 2024) with slight adjustments. Confluent T84 cells were seeded in duplicate sets of six-well Transwell culture inserts at a density of 2.4 \times 10 cells per well, on the membrane surface inside each insert (as described above). Cells were cultured for 7–8 days prior to adhesion experiments. The bacterial strains PAO1 and *L. casei* were washed twice with DPBS. Then 100 μl of PAO1 suspension (10 CFUs) and 100 μl of *L. casei* suspension (10 CFUs) were added simultaneously to each insert. The cultures were incubated at 37 °C for 90 min. After incubation, the monolayers were washed twice with DPBS and digested using TrypLE Express Enzyme. Serial dilutions of adherent bacteria were plated on Luria-Bertani (LB) agar for PAO1 and de Man, Rogosa, and Sharpe (MRS) agar for *L. casei*. Plates were incubated at 37 °C for 24–48 h, after which colon-forming units (CFUs) were counted.

2.13. Statistical analysis

Data analysis was performed using STATGRAPHICS Plus statistical software Version 4.1 (Statgraphics Technologies, Inc., Virginia, USA). All measurements were obtained from in vitro experiments using cultured cells, and results are expressed as mean \pm standard error of the mean (SEM). Each experimental condition was tested in duplicate (technical replicates) within each experiment, and all experiments were independently repeated three times to account for biological variability (e.g., different passages or independently repeated cultures), resulting in a total of six observations per treatment-media group, and 48 observations across all groups. Prior to statistical analysis, data were tested for normality using the Shapiro-Wilk test and for homogeneity of variances using Levene's test. Depending on the data distribution: Comparisons between two groups were perfomed using either Student's t-test (parametric) or the Mann-Whitney U test (non-parametric). Comparisons among multiple groups (i.e., the four treatment groups) were performed using one-way analysis of variance (ANOVA) for normally distributed data) or the Kruskal-Wallis test for non-normally distributed data. When

significant differences were identified, Tukey's HSD test (parametric) or Dunn's test (non-parametric) was used for post hoc pairwise comparisons. A p-value <0.05 was considered statistically significant throughout the study. To ensure adequate statistical power, a power analysis was conducted assuming a medium effect size (Cohen's d =0.5), a significance level of $\alpha=0.05$, and a desired power of 80 % (0.80). The analysis confirmed that the sample size used was sufficient to detect statistically significant differences between treatment groups.

3. Results

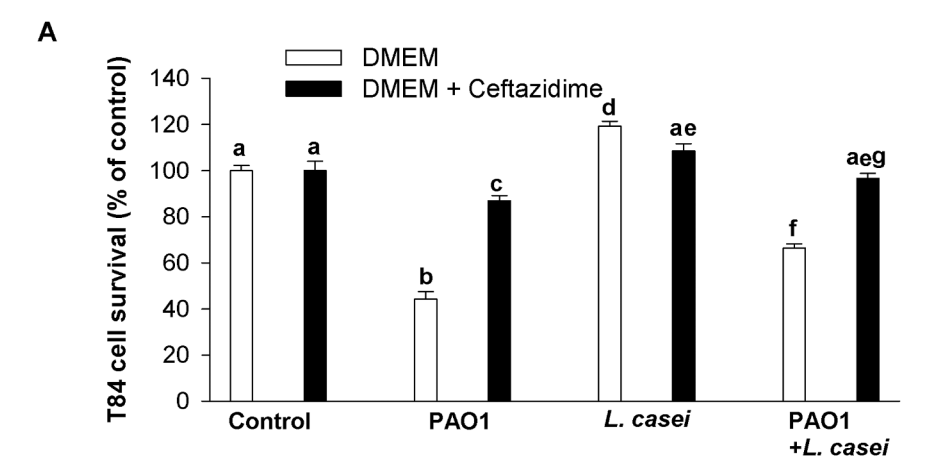
3.1. Cell viability

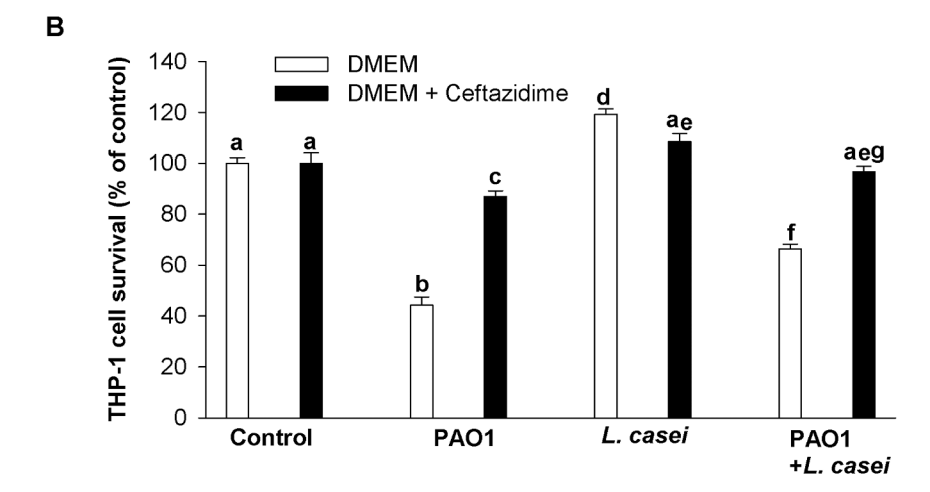
The effects of the tested treatments on the physiological cell health of all three types of co-cultured cells followed a similar pattern, with varying degrees of sensitivity. Exposure of the T84 cell monolayer to PAO1 alone for 6 h significantly (p < 0.01) reduced cell viability to 44.3 \pm 3.0 %) compared to untreated control cells (Fig. 2A). In contrast, treatment with L. casei alone slightly increased cell viability to 109.3 \pm 3.1 %. Thus, unlike PAO1, L. casei maintains optimal physiological cell health without exerting toxic effects on intestinal cells. Moreover, the PAO1-induced reduction in T84 cell viability was significantly (p < 0.01) attenuated by 10.5 % in the presence of L. casei during the 6hour experiment. When co-cultured cells were incubated in DMEM with ceftazidime, the PAO1-induced reduction in cell viability was further inhibited by 30.6 % (p < 0.01). The combination of ceftazidime and L. casei attenuated PAO1-induced cytotoxicity by 33.7 %, compared to L. casei or ceftazidime alone. This indicates that the combination of ceftazidime and L. casei does not exert a synergistic or additive effect on the enhancement of cell viability, as initially anticipated. This lack of an enhanced effect is likely due to the marginal adverse impact of ceftazidime on the growth and survival of L. casei, as reflected in Fig. 7B.

In the case of THP-1 cells, a similar analysis was performed. Treatment with ceftazidime attenuated the PAO1-induced reduction in cell viability by 40.0 % compared to PAO1-treated cells in DMEM alone (Fig. 2B), while treatment with *L. casei* alone resulted in an attenuation of 10.9 %. The combination of ceftazidime and *L. casei* reduced PAO1-induced cytotoxicity by 38.6 % compared to PAO1 alone in DMEM alone. These results imply that THP-1 cells are more sensitive to ceftazidime treatment and, therefore, the combined effect of ceftazidime and *L. casei* is more pronounced inTHP-1 cells than in T84 cells.

The viability of Huh7 cells is shown in Fig. 2C. Treatment with ceftazidime attenuated PAO1-induced decrease in cell viability by 37.6 %. Treatment with *L. casei* alone attenuated the cytotoxic effect by 9.6 %, while the combination of ceftazidime and *L. casei* attenuated it by 34.3 %. These results indicate that although the *L. casei* bacteria did not have direct contact with the Huh7 cells, their secreted beneficial bioactive substances still exerted a protective effect. However, the combined effect of ceftazidime and *L. casei* on Huh7 cell viability was less pronounced than in T84 and THP-1 cells. This difference can be attributed to the interactions between *L. casei*-derived substances and ceftazidime, which can result in reduced bioavailability or efficacy or either component.

Overall, treatment with ceftazidime alone attenuated the PAO1-induced decrease in cell viability by 30.6 % in T84 cells, 40.0 % in THP-1 cells, and 37.6 % in Huh7 cells. Treatment with *L. casei* alone attenuated PAO1-induced cytotoxicity by 10.5 % in T84 cells,10.9 % in THP-1 cells, and 9.6 % in Huh7 cells. Treatment with a combination of ceftazidime and *L. casei* attenuated the PAO1-induced reduction in T84 cell viability by 33.6 % compared to PAO1 in DMEM alone, and by 26.1 % compared to PAO1 plus *L. casei* in DMEM. In THP-1 and Huh7 cells, combined treatment led to attenuations of approximately 27.7 % and 24.6 %, respectively. Although both ceftazidime and *L. casei* have the capacity to counteract PAO1-induced cytotoxicity, their beneficial combined effect does not appear to be additive, as initially anticipated. This lack of synergy may be due to the marginal inhibitory effect of





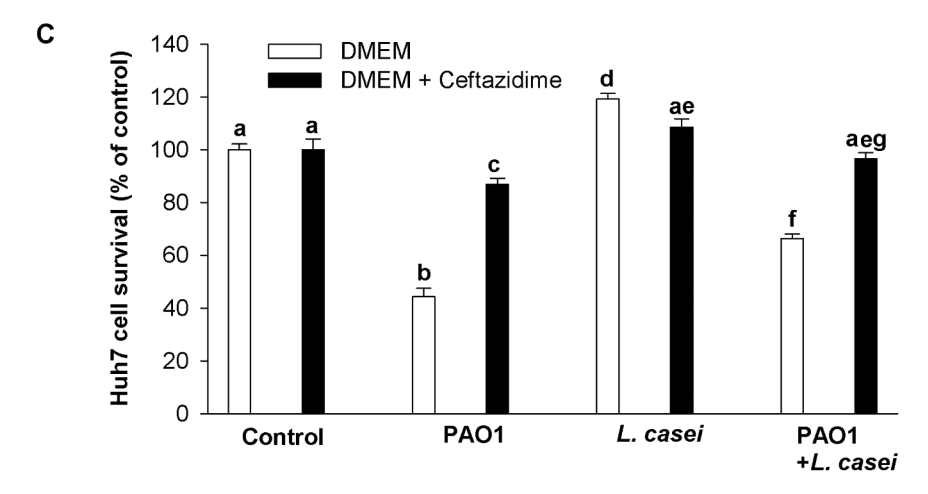


Fig. 2. Viability of T84(panel A), THP-1(panel B), and Huh7(panel C) cells following pathogenic bacterial challenge and subsequent treatment with linoleic acid-producing *Lactobacillus bacteria* (*L. casei*) and ceftazidime. Cell viability was assessed after 6 h of exposure to *P. aeruginosa* PAO1 (MOI 1.7:1) 1 in the presence and absence of *L. casei* and /or ceftazidime, using DMEM alone or DMEM + ceftazidime as the basal medium. The triple co-culture model allowed assessment of viability across epithelial (T84), immune (THP-1), and hepatic (Huh7) compartments. Treatments did not significantly compromise cell viability, indicating that observed cytokine and metabolic changes (see later figures) were not due to overt cytotoxicity. Data are expressed as mean \pm SEM from three independent experiments performed in duplicate. Statistical difference was defined as p < 0.05. Group comparisons among treatments (control, PAO1, *L. casei*, and PAO1 + *L. casei*) within each media condition were assessed using one-way ANOVA. Comparisons between media conditions (DMEM vs. DMEM + ceftazidime) for each treatment group were performed using unpaired Student's *t*-tests. Different letters indicate significant differences between any groups, including both treatment and media condition comparisons. Abbreviations: Control, uninfected cells (without bacteria); PAO1, *Pseudomonas aeruginosa* strain PAO1; *L. casei*, *Lactobacillus casei strain* (ATCC-334).

ceftazidime on the growth and survival of *L. casei* (as reflected in Fig. 7B), or to potential intermolecular interactions between ceftazidime and secreted components derived from *L. casei*. However, further investigations are needed to clarify these mechanisms.

3.2. Protective effect of LA-producing L. casei and ceftazidime against PAO1-induced impairment of intestinal barrier function in T84 cell monolayers

Transepithelial electrical resistance (TEER) is a valuable index for evaluating intestinal barrier integrity (Devriese et al., 2017). As illustrated in Fig. 3, when co-cultured cells were incubated in DMEM alone, PAO1 treatment alone led to a significant decrease in TEER of T84 cells after 6 h, resulting in a TEER value that was reduced by 48.1 % compared to untreated control cells. In contrast, treatment with $L.\ casei$ alone led to an increase in TEER after 6 h (119.2 % compared to untreated control cells). Furthermore, treatment with $L.\ casei$ significantly attenuated the PAO1-induced reduction in TEER by 19.4 % compared to cells treated with PAO1 alone.

When co-cultured cells were incubated in DMEM containing ceftazidime, the PAO1-induced reduction in TEER was significantly inhibited by 45.1 % over the 6-hour experiment. The monolayer of T84 cells treated with L. casei alone for the same duration showed TEER levels almost similar to those of control cells (104.5 %). This indicates that the integrity of the intestinal epithelial barrier function was maintained optimally, without any adverse effects from the L. casei strain on intestinal cells in the triple cell co-culture model. However, when comparing the TEER value with ceftazidime (104.0 %) with the value obtained without it (119.0 %), the TEER was lower in the presence of ceftazidime. This indicates that ceftazidime marginally inhibits the beneficial effects of L. casei. Similarly to the results of the cell viability assays, the combination of ceftazidime and L. casei restored PAO1-suppressed TEER. The combined treatment of ceftazidime and L. casei exhibited a more effective response than either ceftazidime or L. casei alone. However, this effect was not additive, as the combined effects did not equal the sum of each treatment taken separately. These findings support the idea

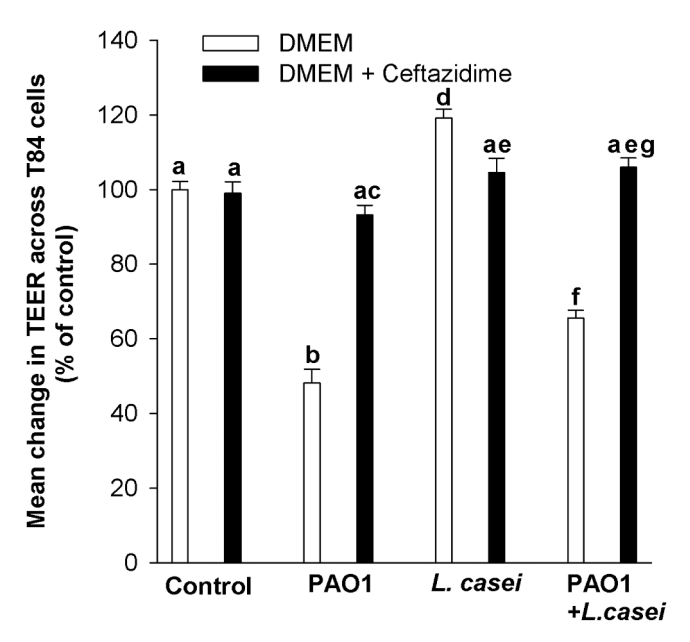


Fig. 3. Effects of linoleic acid-producing Lactobacillus bacteria (L. casei) and ceftazidime on epithelial barrier integrity in T84 cells during P. aeruginosa PAO1 inoculation. Transepithelial electrical resistance (TEER) was measured to evaluate the integrity of T84 epithelial monolayers following 6-hour exposure to P. aeruginosa PAO1 (MOI 1.7:1), with or without L. casei and/or ceftazidime. Treatments were applied in DMEM or DMEM + ceftazidime. TEER values are expressed as % change relative to uninfected control (100 %), with data shown as mean \pm SEM from three independent experiments (each in duplicate). Infection significantly reduced TEER, indicating compromised barrier function, while L. casei and ceftazidime co-treatment partially restored monolayer integrity. Statistical analyses and significance annotations are as described in Fig. 2 legend.

that although ceftazidime and *L. casei* bacteria are effective individually or in combination in alleviating overt infectious inflammation and protecting intestinal epithelial cells by improving the integrity of barrier function in response to pathogen-induced pathological inflammation, their combined effect is not additive. This may be due to the marginal side effect of ceftazidime on *L. casei*, as well as the possibility that ceftazidime and *L. casei* exert their effects through distinct regulated secretory pathways.

3.3. Modulation of protein expression of Th1 and Th2-cytokines associated with integrity of the intestinal barrier during PAO1 challenge

The effects of ceftazidime and the L. casei bacterium, alone or in combination, on the protein secretion of the Th2 cytokine IL-10 and Th1 cytokines IL-1 β and IL-6 from co-cultured T84, THP-1, and Huh7 cells stimulated by the pathogenic PAO1 bacterium are shown in Fig. 4A-C, respectively. The PAO1 bacterium alone resulted in a marked (4.5-fold) decrease in IL-10 protein secretion, while it induced IL-1ß and IL-6 secretion by 8-fold and 5.8-fold, respectively. This aberrant effect of PAO1 on the Th2 to Th1 cytokine response was significantly reduced by ceftazidime, resulting in nearly normal cytokine levels. The L. casei bacterium alone increased the basal secretion of IL-10 and significantly inhibited the PAO1-reduced IL-10 secretion, as shown in Fig. 4B. Conversely, L. casei inhibited the secretion of IL-1ß and IL-6 from cocultured T84, THP-1 and Huh7 cells stimulated by PAO1, as shown in Figs. 4B and 4C. This effect was reinforced by the combination of L. casei and ceftazidime, although it was additive, as expected. Overall, these in vitro results indicate that the balance of Th1 and Th2 cytokine secretion, disrupted by the PAO1 bacterium alone, was modulated by ceftazidime and components secreted by L. casei, since the L. casei bacterium did not have direct access to THP-1 and particularly Huh7 cells. This finding is similar to what has been reported in macrophages, where immunomodulating bioactive factors secreted by lactic acid bacteria (Ren et al., 2020) have similar effects.

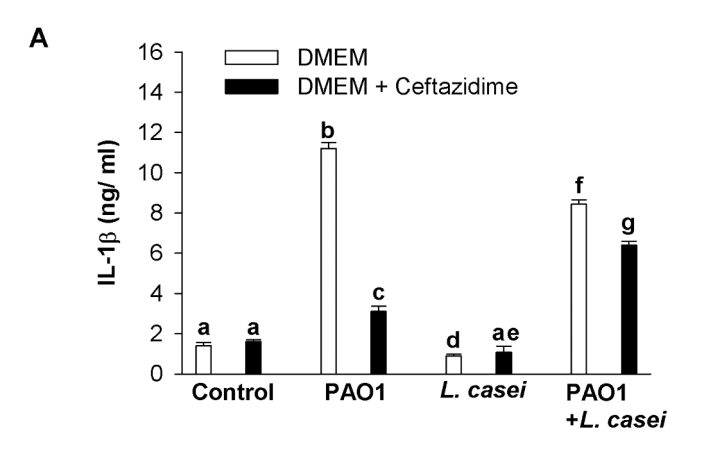
3.4. Modulation of de novo cellular membrane lipids (omega-6) and lipophilic antioxidant (CoQ10) associated with host cell metabolism during PAO1 challenge

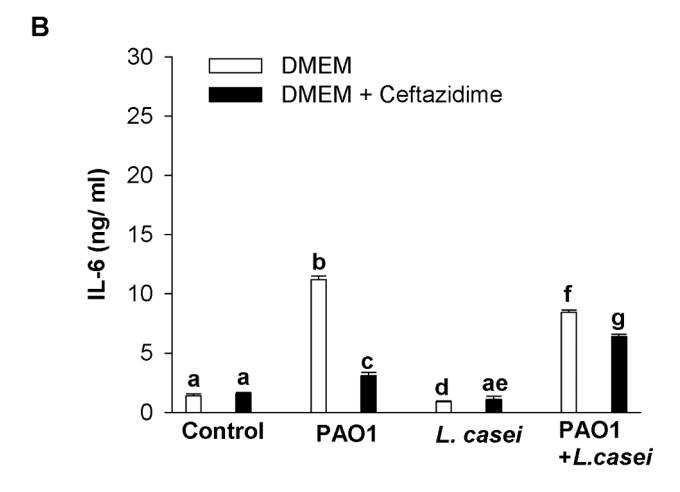
CoQ10 is the only lipid-soluble antioxidant produced by humans, and its solubility protects lipoproteins and lipids from peroxidation and oxidative damage (Lee et al., 2017).

When co-cultured cells were incubated in DMEM alone, the profile of cellular membrane lipids and lipophilic antioxidants associated with host cell metabolism and function showed changed patterns during PAO1 or *L. casei* treatments. The cellular CoQ10 content of the co-cultured T84, THP-1, and Huh7 cells is summarized in Table 1.

When co-cultured cells of T84, THP-1, and Huh7 were incubated with medium alone, the CoQ10 content of cells was markedly reduced in the presence of the PAO1 bacterium alone, while CoQ10 increased in co-cultured cells with the *L. casei* bacterium alone. On the other hand, PAO1-decreased cellular CoQ10 was markedly inhibited in the presence of ceftazidime antibiotic, with the *L. casei* bacterium alone or in combination. However, their combined effect was neither additive nor synergistic, suggesting that complex structural intermolecular bonds (interactions) between ceftazidime and components secreted by the *L. casei* bacterium may occur and play a be critical role in this combined phenotypic effect.

The total cellular omega-6 content of the co-cultured cells is summarized in Table 2, and its pattern closely mirrored that of CoQ10. For example, in the case of intestinal T84 monolayer cells within inserts that had direct contact with tested bacteria for 6 h, cellular levels of CoQ10 and omega-6 were significantly reduced by 5.1 \pm 0.4 and 3.87 \pm 0.10-fold, respectively, after exposure of co-cultured cells to PAO1 alone for 6 h compared to untreated control cells. On the contrary, treatment with the *L. casei* bacterium alone led to an increase in CoQ10 and omega-6





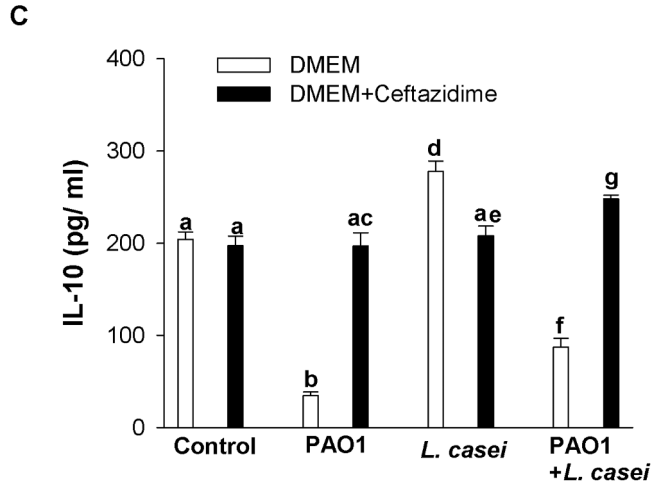


Fig. 4. Linoleic acid-producing *Lactobacillus* (*L. casei*) and ceftazidime modulate cytokine in a human gut–liver co-culture model during bacterial challenge. Protein levels of pro-inflammatory cytokines IL1 β (A) and IL-6 (B), and anti-inflammatory cytokine IL-10 (C) were measured in supernatants from co-cultured T84 (intestinal epithelial cells), THP-1 (macrophages), and Huh7 (hepatocytes) after 6-hour exposure to *P. aeruginosa* PAO1. Treatments included: *L. casei* alone, ceftazidime alone, *L. casei* + ceftazidime, or control medium. The model simulates gut–liver immune responses under infectious-inflamed conditions. Results represent mean \pm SEM from three independent experiments (each in duplicate). Statistical analyses and significance annotations are as described in Fig. 2 legend.

Table 1Cellular CoQ10 content in co-cultured cells treated for 6 h with the *Pseudomonas aeruginosa* strain PAO1, with or without *Lactobacillus casei* bacteria (ATCC 334), in DMEM or DMEM supplemented with ceftazidime.

Cells	Experimental Group	DMEM	${\bf DMEM} + {\bf Ceftazidime}$
T84	Control	6.731 ± 0.371^a	5.922 ± 0.244^{a}
	PAO1	1.153 ± 0.072^{b}	4.611 ± 0.314^{c}
	L. casei	$8.942 \pm 0.611^{\rm d}$	$6.851 \pm 0.377^{\mathrm{e}}$
	PAO1 + L. casei	$3.619 \pm 0.122^{\ f}$	4.194 ± 0.055^{gc}
THP-1	Control	4.412 ± 0.203^a	3.777 ± 0.166^a
	PAO1	0.937 ± 0.044^{b}	4.938 ± 0.402^{c}
	L, casei	5.144 ± 0.118^{d}	$4.622 \pm 0.255^{\rm e}$
	PAO1 + L. casei	$2.809 \pm 0.117^{\ f}$	5.033 ± 0.075 g
Huh7	Control	5.619 ± 0.136^{a}	5.494 ± 0.093^a
	PAO1	$1.101 \pm 0.102^{\rm b}$	4.918 ± 0.206^{c}
	L. casei	6.307 ± 0.099^{d}	4.891 ± 0.179^{e}
	PAO1 + L. casei	$3.111\pm0.081~^{\mathrm{f}}$	4.917 \pm 0.211 $^{\rm g}$

Legend: Coenzyme Q10 levels were measured in co-cultured cells exposed to PAO1 in the presence or absence of L. casei for 6 h. Treatments were conducted in either DMEM or DMEM supplemented with ceftazidime. Results are expressed as pmol CoQ10 per mg of protein (means \pm SEM; n=3 independent experiments, performed in duplicate). Statistical difference was defined as p<0.05. Group comparisons among treatments (control, PAO1, L. casei, and PAO1 + L. casei) within each media condition were performed using one-way ANOVA. Comparisons between media conditions (DMEM vs. DMEM + ceftazidime) for each treatment group were performed using unpaired Student's t-tests. Different letters indicate significant differences between any groups, including both treatment and media condition comparisons. Abbreviations: Control, uninfected cells (without bacteria); CoQ10, Coenzyme Q10; L. casei, Lactobacillus casei strain; PAO1, Pseudomonas aeruginosa strain PAO1; pmol, picomoles.

Table 2Total cellular omega-6 content in co-cultured cells treated for 6 h with the *Pseudomonas aeruginosa* strain PAO1, with or without *Lactobacillus casei* (ATCC 334), in DMEM or DMEM supplemented with ceftazidime.

Cells	Experimental Group	DMEM	$\mathbf{DMEM} + \mathbf{Ceftazi} \; \mathbf{dime}$
T84	Control	8.201 ± 0.189^a	7.859 ± 0.128^{a}
	PAO1	$2.117 \pm 0.101^{\rm b}$	7.222 ± 0.098^{c}
	L. casei	$8.772 \pm 0.311^{\rm d}$	$7.131 \pm 0.277^{\rm e}$
	PAO1 + L. casei	$3.141\pm0.098^{\text{ f}}$	$6.423\pm0.201~^{g}$
THP-1	Control	6.808 ± 0.211^a	6.919 ± 0.088^a
	PAO1	$1.157 \pm 0.107^{\mathrm{b}}$	5.994 ± 0.219^{c}
	L. casei	7.280 ± 0.098^{d}	5.918 ± 0.188^{e}
	PAO1 + L. casei	$2.107\pm0.177~^{\mathrm{f}}$	5.133 ± 0.203 g
Huh7	Control	9.759 ± 0.189^{a}	9.952 ± 0.428^a
	PAO1	$2.519 \pm 0.101^{\rm b}$	8.594 ± 0.108^{c}
	L. casei	$10.438 \pm 0.286^{\rm d}$	8.458 ± 0.263^{e}
	PAO1 + L. casei	$3.197\pm0.208~^{\mathrm{f}}$	$8.943\pm0.201~^{g}$

Legend: Omega-6 levels were measured in co-cultured cells exposed to *Pseudomonas aeruginosa* strain PAO1 in the presence or absence of *L. casei* for 6 h. Treatments were performed in either DMEM or DMEM supplemented with ceftazidime. Data are expressed as pmol of omega-6 per mg of protein (mean \pm SEM; n = 3 independent experiments, performed in duplicate). Statistical difference was defined as p < 0.05. Group comparisons among treatments (control, PAO1, *L. casei*, and PAO1 + *L. casei*) within each media condition were performed using one-way ANOVA. Comparisons between media conditions (DMEM vs. DMEM + ceftazidime) for each treatment group were performed using unpaired Student's *t*-tests. Different letters indicate significant differences between any groups, including both treatment and media condition comparisons. Abbreviations: Control, uninfected cells (without bacteria); *L. casei*, *Lactobacillus casei* strain; PAO1, Pseudomonas aeruginosa strain PAO1; pmol, picomoles.

levels by 1.33 \pm 0.4 and 1.07 \pm 0.3-fold, respectively.

Together, these in vitro results suggest that: Inflammatory, opportunistic pathogenic bacteria, such as PAO1, alter the lipophilic antioxidants of the host cell membrane for their own benefit(advantage); and both ceftazidime and linoleic acid-producing bacteria, such as the *L. casei* bacterium, promote a highly lipophilic antioxidant milieu that can protect against inflammatory bacteria. However, their combined use

does not result in additional beneficial effects.

0,0

Control

PAO1

3.5. Antibiotic a critical arbiter of metabolic host-pathogen interactions affecting glucose

Within host-pathogen metabolic partnerships, four intricate biochemical and microbiological events are closely interconnected: i) Metabolic pathways of sugars, fats, and amino acids interact and are tightly linked to immune cell survival and activation; ii) Host and pathogen compete for glucose and iron during infection, with glucose

utilization also being associated with antibiotic tolerance (i.e., extended exposure time required for antibiotics to be effective); iii) Reprogramming of microbial metabolism depends on nutrient availability, including host-derived lipids; and iv) Infection induces metabolic perturbations within the host cell (Beam et al., 2023; Hu et al., 2022; Tang et al., 2024, 2024; Traven, Naderer, 2019; Troha, Ayres, 2020). Therefore, we measured the levels of glucose, iron, HDL-C, and triglycerides as indicators of host metabolic defense. To assess the glucose consumption rate, the glucose concentration remaining in the medium after 6 h of incubation was quantified for co-cultured cells. As shown in Fig. 5A,

ag

PAO1

+L. casei

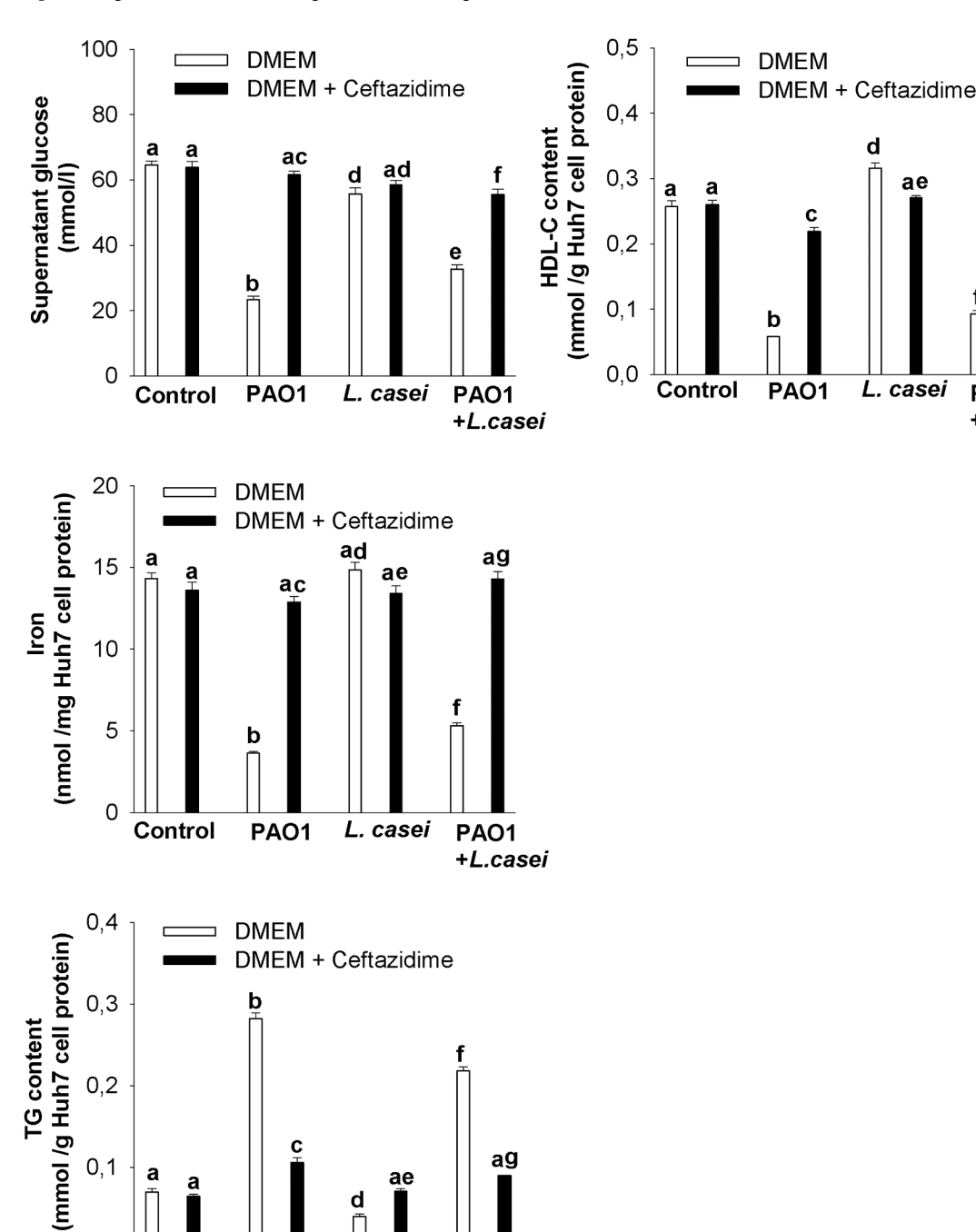


Fig. 5. Metabolic defense indicators in host cells following antibiotic and P. aeruginosa PAO1 inoculation. Glucose (A), iron (B), triglycerides (TG, C), and HDL cholesterol (HDL-C, D) levels were measured in co-cultured T84, THP-1, and Huh7 cells to assess metabolic responses to antibiotic treatment (ceftazidime) and infection with P. aeruginosa PAO1. The metabolic markers reflect the immunopathological changes caused by antibiotic and pathogen exposure. Data are presented as mean \pm SEM from independent experiments (each in duplicate). Statistical analyses and significance annotations are as described in Fig. 2 legend.

PAO1

+L. casei

L.casei

there were no significant differences in basal medium glucose levels when uninfected control cells (without bacteria) were incubated in medium alone or medium supplemented with ceftazidime alone. A glance at Fig. 5A shows that, after 6 h of incubation in DMEM alone, uninfected co-cultured control cells consumed approximately 34 % of the glucose originally present (in DMEM). Note that the initial glucose concentration in the DMEM medium used was 4.5 g/L (equivalent to 97.83 mmol/L). Supplementing DMEM with the antibiotic ceftazidime resulted in a slight increase in cellular glucose consumption, as evidenced by lower glucose levels in the supernatant, although this difference was not statistically significant. In contrast, infection with the PAO1 bacterium caused a significant reduction in glucose levels in the culture medium. This glucose-depleting effect was inhibited in the presence of ceftazidime, indicating that PAO1 infection activates host cell glycolysis and enhances cellular glucose uptake. Increased glucose uptake is not only an intrinsic hallmark of most cancer cells, but is also a characteristic of host cells infected by bacterial pathogens (Tang et al., 2024, 2024). Interestingly, unlike many pathogenic bacteria, P. aeruginosa preferentially utilizes organic acids or amino acids over glucose as energy sources, a strategy linked to its infection-driven modulation of host metabolism (Tang et al., 2024, 2024). Therefore, observed glucose consumption likely reflects increased metabolic activity and glucose utilization by infected host cells rather than by the bacteria themselves. On the other hand, when cells were incubated in DMEM medium alone, treatment with the L. casei bacterium alone did not significantly alter glucose levels in the medium compared to untreated control cells, despite the fact that *L. casei* itself consumes glucose. However, in the presence of ceftazidime, glucose levels in L. casei-treated cell media decreased significantly compared to DMEM without ceftazidime. These results indicate that: i) P. aeruginosa PAO1 and L. casei bacteria exert opposite effects on host cell glucose metabolism; and ii) Antibiotics and bio-immune modulators (such as beneficial bacteria) can have paradoxical and bidirectional effects—some of which may be therapeutically beneficial, while others may lead to unintended consequences. In this context, the crosstalk and interplay between cellular iron and glucose metabolism at the host-pathogen interface are more complex than previously imagined, often resulting in multiple physiological changes in both biologically active actors (host and pathogen) within that interface (Troha, Ayres, 2020).

Among other metabolic defense indicators, we focused on the cellular iron, TG, and HDL-C content of Huh7 cells, although our model consists of three cell types. This focus is due to the central role of the liver in maintaining systemic iron homeostasis through three essential functions: 1) it is the main site for the production of proteins that maintain and regulate systemic iron balance, 2) it serves as a storage site for excess iron, and 3) it plays a critical role in mobilizing iron from hepatocytes into the circulation to meet metabolic requirements (Anderson and Shah, 2013). Moreover, the liver is the main organ responsible for synthesizing TG and HDL-C, bio-distributing lipids throughout the circulation, and detoxifying circulating bacterial LPS (endotoxin). The analysis of cellular iron content is shown in Fig. 5B. Compared to the untreated control group (14.31 \pm 0.34 nmol/mg of cellular protein), the iron content in the PAO1-treated group was significantly reduced (3.62 \pm 0.38 nmol/mg of cellular protein). Conversely, treatment with the L. casei slightly increased the iron content, although the difference was not statistically significant. This marginal induction is likely because lactic acid bacteria are among the few microorganisms that do not require iron for growth, even in the presence of ferritin or other forms of iron storage. Additionally, their lactic acid increases iron bioavailability for eukaryotic host cells (García-Mantrana et al. 2025). Co-treatment with PAO1 and L. casei inhibited the PAO1-induced decrease in iron content, indicating a protective effect compared to PAO1 treatment alone.

When co-cultured cells were incubated in DMEM containing ceftazidime, Huh7 cells exhibited a marked increase in iron levels compared to those treated with PAO1 bacterium alone (12.88 \pm 0.33 vs. 3.63

 \pm 0.38 mmol/g of cellular protein). Ceftazidime treatment also interfered with the effect of $L.\ casei$ on iron content. Notably, co-treatment with both ceftazidime and $L.\ casei$ further prevented the PAO1-induced reduction in iron content compared to treatment with either ceftazidime or $L.\ casei$ alone. Taken together, these results indicate that modulation of immunometabolic responses within the gut–liver axis—and the efficacy of antibiotic treatment during infection—depend not only on host nutrient availability (particularly glucose and iron), but also on the convergent interactions between host cells and beneficial bacteria in counteracting invading pathogens at the site of infection.

The cellular triglyceride (TG) content, another key indicator of metabolic defense in host cells, is shown in Fig. 5C. When co-cultured cells were incubated in DMEM alone, TG levels in PAO1-treated Huh7 cells were significantly elevated compared to the control group (0.071 \pm 0.004 vs. 0.282 \pm 0.073 mmol/g of protein). Treatment with *L. casei* alone resulted in a reduction in content, although the decrease was not statistically significant. However, compared to the PAO1-alone group, *L. casei* effectively inhibited the PAO1-induced increase in TG levels (0.218 \pm 0.0052 vs. 0.282 \pm 0.073 mmol/g of cellular protein).

When co-cultured cells were incubated in DMEM supplemented with ceftazidime, as expected, the antibiotic significantly attenuated the PAO1-induced increase in TG content (0.106 \pm 0.0061 vs. 0.282 \pm 0.073 mmol/g of cellular protein). When comparing control cells to those treated with *L. casei* alone, *L. casei* significantly decreased the basal TG content in Huh7 cells within the co-culture system incubated in DMEM. Interestingly, this effect was inhibited in the presence of ceftazidime (0.071 \pm 0.0031 vs. 0.061 \pm 0.031 mmol/g of cellular protein) (Fig. 5C). Co-treatment with ceftazidime and *L. casei* further inhibited the PAO1-increased elevation of TG levels (0.139 \pm 0.0071 vs 0.218 \pm 0.055 mmol/g of cellular protein); however, this effect was not additive when compared to treatment with either *L. casei* or ceftazidime alone.

Analysis of cellular HDL-C content is shown in Fig. 5D. When cocultured cells were incubated in DMEM alone, HDL-C levels in Huh7 cells were significantly reduced in the PAO1-treated group compared to the untreated control (0.058 \pm 0.007 vs 0.257 \pm 0.092 mmol/g of cellular protein) in Huh7 cells. Treatment with *L. casei* alone led to a moderate increase in HDL-C levels compared to the untreated control group. Notably, *L. casei* also inhibited the PAO1-induced decrease in HDL-C levels when compared to cells treated with PAO1 alone.

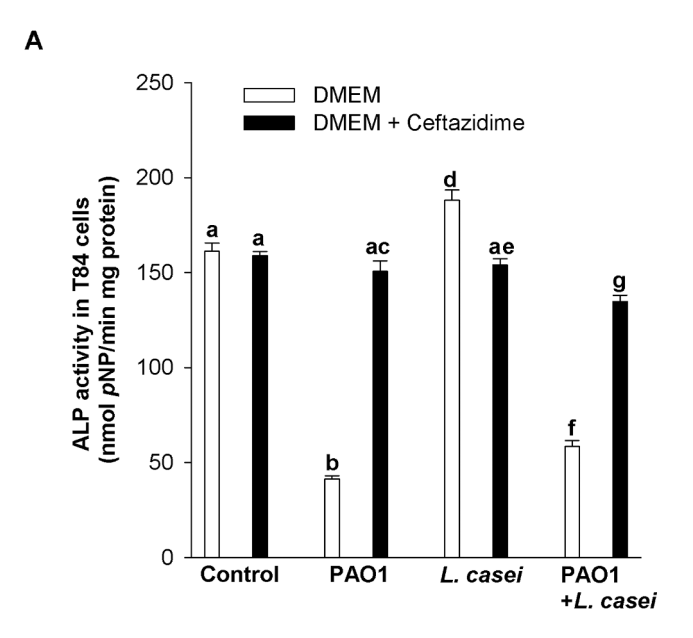
As expected, incubation of co-cultured cells in DMEM supplemented with ceftazidime significantly reversed the PAO1-induced reduction in HDL-C levels, showing a 3.8-fold increase compared to the PAO1- alone group. Conversely, ceftazidime reduced the $\it L. casei$ -induced increase in HDL-C by approximately 10 % compared to the group treated with $\it L. casei$ alone. The combination treatment of $\it L. casei$ and ceftazidime further prevented the PAO1-induced decrease in HDL-C more effectively than either treatment alone.

As with other aspects of the host response, a glance at Fig. 5C-D collectively illustrates that ceftazidime and linoleic acid-producing *L. casei* strain can improve lipid metabolism in PAO1-treated Huh7 cells. Importantly, although *L. casei* did not have direct access to Huh7 cells in our co-culture model, its secreted metabolites were able to modulate both pro- and anti-inflammatory lipid mediators in this liver-derived cell line. The liver, being the central organ for lipid synthesis, biodistribution, and homeostasis, plays a key role in this interaction. However, it is also evident that *L. casei* is not fully resistant to the marginal adverse side effects of ceftazidime treatment.

3.6. Modulation of alkaline phosphatase activity as a hallmark of antibiotic-induced intestinal dysbiosis and a key intestinal mucosal defense enzyme

Among body organs, changes in liver and, particularly, intestinal alkaline phosphatase (AP) activity are hallmark of antibiotic-induced

intestinal dysbiosis. Intestinal AP plays a critical role in preventing antibiotic-induced susceptibility to enteric pathogens, detoxifying lipopolysaccharide (LPS), regulating intestinal microbiota, and exerting anti-inflammatory effects via the Toll-like Receptor-4 (TLR-4) signaling pathway (Dissanayake et al., 2023; Estaki et al., 2014). As shown in Figs. 6A and 6B, there were no significant differences in AP activity in T84 and Huh7 cells when uninfected control cells were incubated in either medium alone or medium supplemented with ceftazidime. However, infection with PAO1 alone caused a significant decrease in AP activity in both cell lines. This reduction was prevented by ceftazidime



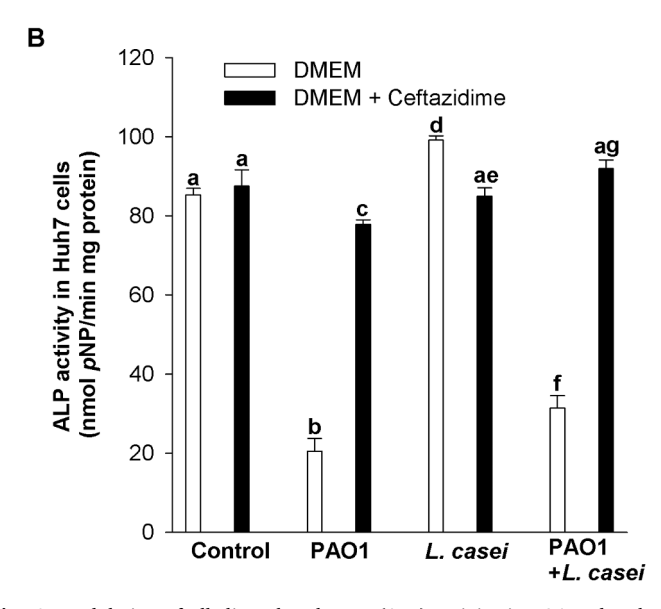


Fig. 6. Modulation of alkaline phosphatase (ALP) activity in T84 and Huh7 cells following antibiotic treatment and *P. aeruginosa* PAO1 infection. ALP activity was measured in the lysates of T84 cell (**A**) and Huh7 (**B**) cells after a 6-hour incubation with either uninfected controls or *P. aeruginosa* PAO1 (MOI 1.7:1) in the presence or absence of 1 mg/ml ceftazidime. ALP activity serves as a marker of intestinal mucosal defense and dysbiosis induced by antibiotic treatment. Data are represented as mean \pm SEM from three independent experiments performed in duplicate. Statistical analyses and significance annotations are as described in Fig. 2 legend.

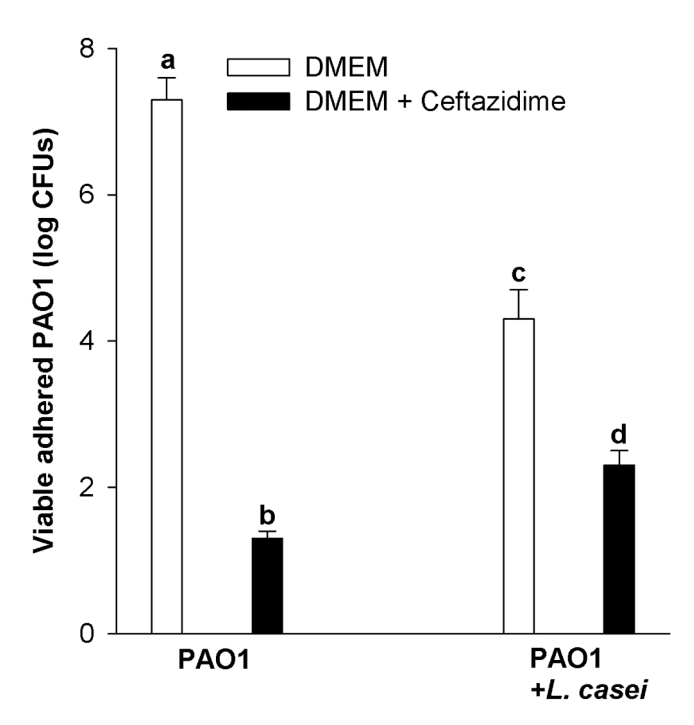
treatment, implicating the direct action of pathogen-secreted signal molecules in reducing AP activity and manipulating the immune response to disrupt host defense enzymes, including gut mucosal enzymes. Conversely, treatment with the *L. casei*, a bacterium known to produce linoleic acid (Peng et al., 2018), significantly increases AP activity in both T84 and Huh7 cells. It also counteracted the PAO1-induced reduction in AP activity in both cell types. However, this protective effect was slightly abolished when cells were co-treated with ceftazidime, suggesting a marginal adverse effect of the antibiotic on the biological activity of *L. casei*. Overall, these results support previous in vivo studies showing that lactic acid bacteria enhance intestinal IAP activity *in vivo* (Goudarzi et al., 2024; Mohanty et al., 2019).

3.7. Concomitant effects of ceftazidime and L. casei bacterium on the growth and survival of PAO1

We next evaluated the anti-adhesion effects of the linoleic acidproducing L. casei bacterium against the PAO1 pathogen using a competition assay. As shown in Fig. 7A, when PAO1 bacteria alone were added to T84 cells in DEMEM alone, an average of 7.3 log CFUs of PAO1 was remained after washing with DPBS. Note that T84 cells were treated with 10⁸ CFUs of PAO1. As expected, treatment with the antibiotic ceftazidime alone markedly reduced PAO1 counts, with an average of 1.3 log CFUs, compared to 7.3 log CFUs in untreated cells. Inoculation with the L. casei bacterium alone also significantly reduced the number of PAO1 bacterial cells adhering to T84 cells. In this condition, the average PAO1 count were 4.3 log CFUs, compared to 7.3 log CFUs in the PAO1-only group. A further reduction in PAO1 survival was observed with the combined treatment of ceftazidime and L. casei. Specifically, the combination resulted in an average of 2.8 log CFUs of PAO1 adhering to T84 cells, lower than with L. casei alone (4.3 log CFUs). However, the anti-adhesion effect of the combined treatment was neither additive nor synergistic, contrary to expectation. These results suggest that linoleic acid produced by the L. casei bacterium interferes with PAO1 adhesion factors, thereby preventing its attachment to T84 cells. This beneficial property appears to be modestly impaired by the adverse side effects of ceftazidime. Overall, these data highlight the cytoprotective potential of both ceftazidime and L. casei when used in co-culture with T84cells against PAO1 infection. In parallel, Fig. 7B illustrates the marginal adverse effect of ceftazidime on L. casei survival and adhesion during a 90-minute competition assay within our inflamed co-culture model. Over this period, the reduction in L. casei survival in DMEM alone was negligible (a 3.37 % decrease; 7.73 log CFUs vs. 8 log CFUs initially added). However, in DMEM containing ceftazidime, L. casei survival decreased by approximately 16.43 % (6.1 log CFUs vs. 7.3 log CFUs). In other words, treatment with the ceftazidime reduced the average number of L. casei adhering to T84 cells. When co-inoculated with PAO1 in DMEM alone, L. casei survival was reduced by approximately 5.06 % (6.93 log CFUs vs. 7.3 log CFUs). This reduction was further exacerbated in the presence of PAO1 and ceftazidime, resulting in an average of 5.3 log CFUs of L. casei retained after DPBS washing (compared to 7.3 log CFUs). These data indicate that in an infectious inflammatory milieu, antibiotics such as ceftazidime may have dual effects, beneficial or detrimental, depending on various factors, including nutrient competition, dosage, and the number and types of bacteria present. Supporting this, previous studies have shown that lactic acid bacteria exhibit variable resistance to ceftazidime (standard concentration 30 µg/ml), depending on whether the resistance is intrinsic or acquired (Duche et al., 2023). Therefore, we employed a clinically relevant dose of ceftazidime (1 mg/ml) to target PAO1 in our infectious-inflamed intestinal model.

4. Discussion

In our experimental model simulating an infectious-inflamed gutliver axis milieu, we observed the beneficial and cytoprotective effects



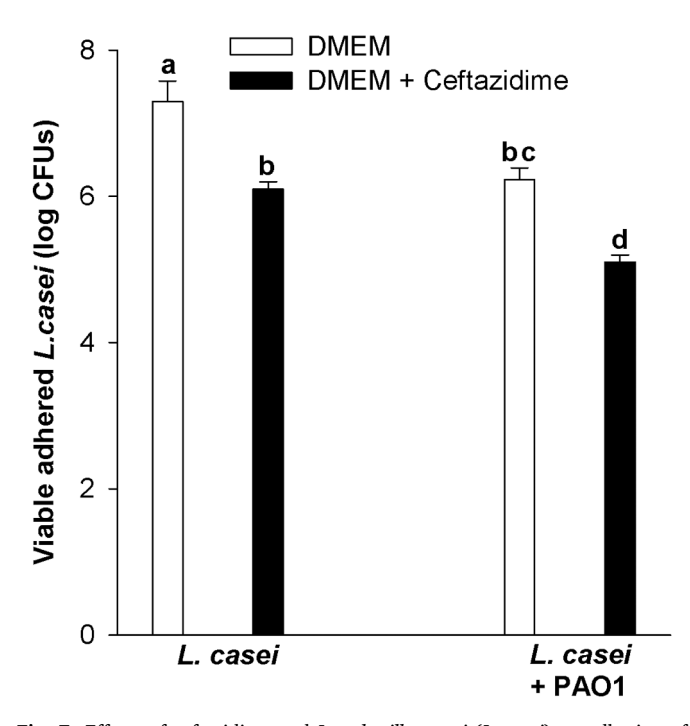


Fig. 7. Effects of ceftazidime and *Lactobacillus casei* (*L. casei*) on adhesion of *P. aeruginosa* PAO1 to T84 intestinal epithelial cells. Polarized T84 monolayers were incubated with *P. aeruginosa* PAO1 (control) or co-incubated with *Lactobacillus casei* (10⁸ CFUs) for 90 min in either DMEM or DMEM supplemented with 1 mg/ml antibiotic ceftazidime. After washing (twice with DPBS) and digestion (using TrypLE Express Enzyme), adherent bacteria were counted by plating serial dilutions on LB and MRS agar for *P. aeruginosa* PAO1 and *L. casei*, respectively. The number of viable bacteria (CFUs) adhered to T84 cells was assessed after 24–48 h of incubation at 37 °C. *P. aeruginosa* PAO1 CFUs (A) and *L. casei* CFUs (B) are shown. Data are presented as mean ± SEM from three independent experiments (each in duplicate). Statistical analyses and significance annotations are as described in Fig. 2 legend.

from the combined treatment of antibiotic ceftazidime and LAproducing L. casei bacteria against the pathogenic PAO1 strain. Overall, PAO1 and L. casei exerted opposite effects on the secretion of the Th1 cytokines IL-1\beta and IL-6, as well as the Th2-type cytokine IL-10, by cocultured T84, THP-1 and Huh7 cells. In co-cultures treated with PAO1 alone, significant inverse correlations were observed between CoQ10 levels and pro-inflammatory cytokines IL-1 β and IL-6, alongside positive correlation with IL-10, TEER, and cell viability. A similar pattern was also observed for total cellular omega-6 linoleic acid levels. Notably, simultaneous treatment with PAO1 and L. casei improved the cellular response to pathogen, as manifested by increased cell viability and enhanced TEER values, both indicators of improved cell health and biofunctionality. Ceftazidime exhibited dual effects in this context. While it alleviated the toxic effects of PAO1 on biochemical markers and oxidative stress, it also marginally disrupted the beneficial effects of L. casei. These findings suggest a complex interaction between antibiotic treatment and beneficial microbial activity, influenced by the inflammatory milieu and microbial competition. In this context, both CoQ10, a fat-soluble antioxidant, and omega-6 linoleic acid and its metabolic derivatives play essential roles in the integrity of phospholipid membranes and the overall cellular defense system. CoQ10, the only lipidsoluble antioxidant endogenously synthesized by humans, is known to protect lipoproteins and lipids from peroxidation and oxidative damage (Lee et al., 2017; Zou et al., 2022).

At the metabolic defense level, we observed that the combined effects of ceftazidime and LA-producing *L. casei* inhibited PAO1-induced disruptions in cellular glucose, iron, and triglyceride metabolism, while simultaneously enhancing levels of the key anti-inflammatory lipid, HDL-C.

Among cytokines, an impaired Th1/Th2 balance often results from a mismatched between systemic bacterial toxin input (translocation) and toxin output (via hepatic detoxification). Reducing toxin input while enhancing detoxification capacity is key to normalizing or maintaining Th1/Th2 cytokine homeostasis and alleviating the related inflammatory burden (Albillos et al. et al., Dissanayake et al., 2023; Estaki et al., 2014). Of the Th1/Th2 biomarkers we evaluated, IL-10 is strongly associated with protective functions, particularly in maintaining intestinal barrier integrity and preventing epithelial hyperpermeability. In contrast, IL-1 β and IL-6 are multifunctional pro-inflammatory cytokines that play central roles in diverse physiological and pathological pathways and inflammation, especially those related to pathological inflammation (Vebr et al., 2023).

With regard to the host's antioxidant and anti-inflammatory lipid defenses, our results of improved cellular CoQ10 and omega-6 contents are supported by recent evidence. According to the inflammatory index, omega-6 fatty acids are classified among anti-inflammatory dietary components, and CoQ10 has demonstrated both anti-inflammatory and antioxidant properties in the context of infectious diseases, as shown in preclinical and clinical studies (Poli et al., 2023; Sifuentes-Franco et al., 2022).

Regarding the biological activity of secreted surface components and metabolites of lactic acid bacteria within the gut–liver axis under inflammation conditions, both in vitro and in vivo studies have demonstrated that lactic acid bacteria and their secreted soluble factors can enhance the secretion of biologically active human anti-inflammatory cytokines (e.g., IL-10), while simultaneously reducing the secretion of pro-inflammatory cytokines (e.g., IL-1 β , IL-6). Additionally, they have been shown to protect against intestinal injury caused by pathogenic bacteria and their LPS through the modulation of host transcription factors. These functions have been well reviewed elsewhere (Liu et al., 2020; Llewellyn, Foey, 2017).

Our results indicate a potential link between improper antibiotic usage, nutrients status dysregulation, depletion, and immunometabolic disturbance under infectious-inflamed milieus. Impaired autophagy and oxidative stress may be key conceivable mechanisms, since dysregulated β -cell autophagy contributes to type 2 diabetes (T2DM) development.

CoQ10 has been shown to improve endothelial function and reduce inflammation (Al-Kuraishy et al., 2019 and Al-Kuraishy et al. 2024), and its supplementation combined with metformin improves endothelial function and reduces inflammatory markers, probably through autophagic modulation. Medications such as antibiotics and metformin may also influence nutrient status and metabolic risk (Al-Kuraishy et al., 2019; Mantle and Golomb, 2025), highlighting the need to incorporate nutrition-focused strategies into the pharmacological segment and consider nutrient—drug interactions. In this sense, although our study was conducted in vitro, it may provide insight for future in vivo explorations and pave the way for further research in living models in the context of metabolic dysregulation in T2DM.

At the molecular and cellular levels, our results align with previous studies showing similar effects on cell viability and signaling pathways. For instance, Abi Nahed et al. (2025), Aditya et al. (2025), Gross et al. (2024), Liu et al. (2023), Liu et al. (2025), Peng et al. (2018), and Taitz et al. (2025) reported comparable outcomes in both in vitro and *in vivo* models, supporting our observations. Furthermore, recent studies (Mantle and Golomb, 2025; Sifuentes-Franco et al., 2022; Xu et al., 2025) further highlight the biological roles of CoQ10 and omega-6 in infectious and chronic diseases, strengthening the biological relevance of our results. Recent literature further supports the beneficial effects of CoQ10 and omega-6 in mitigating antibiotic-induced inflammation, particularly by modulating the immune pathways, the intestinal microbiota, and chronic inflammation. These studies contextualize the anti-inflammatory effects of CoQ10 and omega-6 on antibiotic-, and dysbiosis-induced damage, illustrating how these compounds may

target underlying causes of pathological inflammation, such as mitochondrial dysfunction, immune regulation, and microbial imbalance (Acosta and Alonzo, 2022; Gross et al., 2024; Mantle and Golomb, 2025; Perdijk et al., 2024; Taitz et al., 2025).

Overall, an evaluation of cell viability and functionality in our infectious-inflamed co-culture model reveals two key points: (1) the beneficial and partially synergistic cytoprotective effects of LA-producing *L. casei* and ceftazidime, and (2) while ceftazidime helps the competitive growth of LA-producing bacteria and is effective in controlling infections, it also poses a marginal the risk of inadvertently targeting beneficial LA-producing strains in the gut. The ultimate outcomes are likely influenced by host nutrient availability, the dosage of antibiotic (e.g., ceftazidime) used, and the type and burden of pathogenic bacteria present.

The proposed cellular and molecular mechanisms underlying the beneficial, combined cytoprotective effects of ceftazidime and LA-producing *L. casei* are schematically illustrated in Fig. 8. In summary: (i) inhibition of pathogenic PAO1 adhesion to epithelial cells, thereby preventing disruption of intestinal epithelial cell homeostasis and reducing the risk of intestinal epithelial barrier dysfunction; (ii) induction of protective lipid accumulation in host cell membranes and enhancement of antioxidant defense molecules, such as CoQ10 and omega-6, which contribute to the protection of host cells, tissues, and organs following infection, primarily as a response to damage caused by the growth and metabolic byproducts of infectious agents (reviewed in (Sifuentes-Franco et al., 2022); and (iii) restoration of the dysregulated Th1/Th2 cytokine balance, supporting a more controlled and effective

Pathogen-host interface Antibiotic Pseudomonas aeruginosa PAO Absorptive, defense, and Linoleic acids-producing metabolic cell compartments Lactobacillus casei Macrophage-like THP-1 Cells Huh7 Hepatocytes metabolize, detoxify, and inactivate exogenous toxic molecules such as LPS. PAO1 pathogenicity: Coupled with aberrant Th1/Th2 cytokine ratio, disrupted host metabolic defense (glucose, iron, HDL-C), and reduced host lipid/antioxidant defense (Omega-6/CoQ10).

Modulatory effects of ceftazidime and linoleic acid-producing Lactobacillus casei on the outcome of pathogen-host interactions

Fig. 8. Proposed mechanisms of the cytoprotective effects of ceftazidime and linoleic acids producing *Lactobacillus casei* (*L. casei*). This diagram illustrates the combined effects of ceftazidime and *L. casei* on host immunity and pathogen adhesion. *P. aeruginosa* PAO1 adheres directly to host cells (**bold red sharp arrow**). Ceftazidime directly inhibits the growth of the *P. aeruginosa* PAO1 (**bold blunt arrow**), making it easier for LA-producing *L. casei* to compete, but it also exerts a mild inhibitory effect on *L. casei* (**long thick blunt arrow**), marginally reducing its growth. *L. casei* enhances host cell defense by increasing cellular lipid and antioxidant defense molecules (**thick red sharp arrow** \rightarrow), while reducing PAO1 adhesion through competition exclusion (**short thick blunt arrow**). The interplay between antibiotic and *L. casei* highlights both protective and marginal adverse effects: ceftazidime at the tested concentration effectively inhibits PAO1 growth but slightly interferes with *L. casei* (**weak blunt arrow**). This may be due to concentration or exposure duration, or to differential molecular mechanisms (e.g., ceftazidime–receptor competition), and warrants further investigation. Overall, the diagram illustrates the complexity of nutrient–pathogen–antibiotic interactions. **Legend**: Red sharp arrows (\rightarrow) indicate stimulation; blunt arrows ($^{\perp}$) indicate inhibition.

immune response under infectious and pathological inflammatory conditions.

4.1. Limitations and confounding factors

This study was conducted using an in vitro cell co-culture model, which provides a controlled environment to investigate bacterial interactions, antibiotic responses, and nutrient-antibiotics interactions. However, such models have inherent limitations. They do not fully replicate the complexity of in vivo systems, including host immune responses, tissue-specific microenvironments, and the pharmacokinetics and pharmacodynamics of antibiotic. As a results, the physiological relevance of the results may be limited, and caution should be exercised when extrapolating the results to clinical scenarios. Several potential confounding factors may also influence the observed outcomes. These include variability in culture conditions such as media composition, oxygen availability, and incubation parameters, all of which can affect bacterial growth, metabolism, and antibiotic susceptibility. In addition, batch-to-batch variation in reagents, as well as differences in the behavior of specific cell lines, bacterial strains or nutrients (deficiency or excess), may contribute to experimental variability. While we employed standards protocols and used reagents from the same production lots, where possible to minimize such effects, some degree of variability is unavoidable. Further studies incorporating more physiological relevant models, including in vivo systems, are needed to validate and expand upon these results. Further investigations at the cellular and molecular levels will be also be important to fully elucidate the mechanisms underlying the observed results. Regarding practical implications, the observed interactions between bacterial species under co-culture conditions suggest that polymicrobial environments and bacteria-nutrients interactions may influence antibiotic efficacy in clinically relevant ways. This highlights the importance of considering microbial community dynamics (not just individual pathogens) when selecting antimicrobial therapies. In addition, the differential response to antibiotics in co-culture versus monoculture underscore the potential limitations of standard in vitro susceptibility testing, which typically uses singlespecies models. These results suggest that incorporating polymicrobial considerations into susceptibility testing may improve treatment accuracy, particularly in infections known to involve multiple species, such as chronic wounds, respiratory infections, or biofilm-associated infections. Finally, our result may provide future development of combination therapies or targeted interventions that account for interspecies interactions, potentially improving clinical outcomes in complex infections.

4.2. Conclusion

At the host-pathogen interface, Pseudomonas aeruginosa PAO1 and linoleic acid (LA)-producing lactic acid bacteria exert opposite effects on the immune response, viability, and biofunctionality of host cells. Antibiotics such as ceftazidime intervene in these biochemical processes, and key host-derived nutrients-CoQ10 and omega-6 fatty acids-appear to play central roles in modulating these interactions. Our results suggest that pathogenic and LA-producing bacteria may differentially insert effector molecules into the host phospholipid membranes, hijacking host cellular machinery in distinct ways. In the context of the gut-liver axis, linoleic acid-producing bacteria and antibiotics were found to modulate host metabolic defense mechanisms, influencing glucose metabolism, membrane lipid composition, and antioxidant responses. These interactions collectively contribute to the modulation of colonic immunometabolic responses during P. aeruginosa PAO1 infection and may reduce disease severity and pathological inflammation. However, antibiotic outcomes can be either beneficial or negative outcomes depending on multiple factors, including nutrient availability, the nutrient competitors, bacterial composition, antibiotic dosage, and the type of antibiotic resistance (primary or secondary) of LA-producing bacteria present at the infection sites (Anderson et al., 2010; Vliex et al., 2024). To build on these results, future studies should focus on validating these mechanisms in vivo using in vivo models that recapitulate host-microbe-nutrient interactions within the gut-liver axis. Additionally, further studies are needed to dissect the molecular pathways by which LA-producing bacteria influence host membrane composition and immune signaling. It will also be important to explore how different antibiotic regimens affect host-microbe-nutrient interactions in polymicrobial infection settings. These directions may ultimately inform more precise therapeutic strategies that account for microbial ecology and host nutritional status.

Ethical considerations (obtaining informed consent)

Not applicable. This study has been done only in in vitro cell culture models

Funding

The authors did not receive any type of external funding for the present work.

CRediT authorship contribution statement

Darab Ghadimi: Writing - review & editing, Writing - original draft, Validation, Methodology, Investigation, Formal analysis, Data curation, Conceptualization. Sophia Blömer: Writing – original draft, Validation, Methodology, Investigation, Formal analysis, Data curation, Conceptualization. Christoph Röcken: Writing - review & editing, Writing original draft, Supervision, Methodology, Conceptualization. Heiner Schäfer: Writing – review & editing, Writing – original draft, Validation, Supervision, Methodology, Conceptualization. Aysel ŞAHİN KAYA: Writing - review & editing, Writing - original draft, Validation, Supervision, Methodology, Conceptualization. Sandra Krüger: Writing - review & editing, Writing - original draft, Validation, Methodology, Investigation, Conceptualization. Wilhelm Bockelmann: Writing - review & editing, Writing - original draft, Validation, Supervision, Methodology, Investigation, Formal analysis, Conceptualization. Jumpei Uchiyama: Writing – review & editing, Writing – original draft, Supervision, Methodology, Investigation, Conceptualization. Shigenobu Matsuzaki: Writing - review & editing, Writing - original draft, Validation, Supervision, Methodology, Investigation, Conceptualization.

Declaration of Competing Interest

The authors declare that they have no known competing financial interests or personal relationships that could have appeared to influence the work reported in this paper.

Acknowledgments

The authors would like to thank A. Thoss and N. Timm for helpful technical assistance.

Animal study statements

Not applicable. This study has been done only in in vitro cell culture models

Data availability

Data will be made available on request.

References

- Abi Nahed, R., Hussein, A., Cottet-Rousselle, C., Vogelsang, A., Aulicino, F., Berger, I., Blatt, T., Weise, J.M., Schlattner, U., 2025. Coenzyme Q10 protects keratinocytes against oxidation-induced energy stress as revealed by spatiotemporal analysis of cell energetics. Sci. Rep. 15 (1), 14501.
- Acosta, I.C., Alonzo 3rd, F., 2022. Antibiotic treatment ignites a fire that lasts. Cell Host Microbe 30 (7), 897–899.
- Aditya, A., Tabashsum, Z., Martinez, Z.A., Biswas, D., 2025. Effects of Metabolites of Lactobacillus casei on Expression and Neutralization of Shiga Toxin by Enterohemorrhagic Escherichia coli. Probiotics Antimicrob. Proteins 17 (3), 1466–1472.
- Albillos, A., de Gottardi, A., Rescigno, M., 2020. The gut-liver axis in liver disease: Pathophysiological basis for therapy. J. Hepatol. 72 (3), 558–577.
- Al-Kuraishy, H.M., Al-Gareeb, A.I., Shams, H.A., Al-Mamorri, F., 2019. Endothelial dysfunction and inflammatory biomarkers as a response factor of concurrent coenzyme Q10 add-on metformin in patients with type 2 diabetes mellitus. J. Lab. Physicians 11 (04), 317–322.
- Al-Kuraishy, H.M., Jabir, M.S., Al-Gareeb, A.I., Klionsky, D.J., Albuhadily, A.K., 2024. Dysregulation of pancreatic β-cell autophagy and the risk of type 2 diabetes. Autophagy 20 (11), 2361–2372.
- Anderson, E.R., Shah, Y.M., 2013. Iron homeostasis in the liver. Compr. Physiol. 3 (1), 315–330.
- Anderson, R., Tintinger, G., Cockeran, R., Potjo, M., Feldman, C., 2010. Beneficial and harmful interactions of antibiotics with microbial pathogens and the host innate immune system. Pharmaceuticals 3 (5), 1694–1710.
- Baker, L.Y., Hobby, C.R., Siv, A.W., Bible, W.C., Glennon, M.S., Anderson, D.M., Symes, S.J., Giles, D.K., 2018. Pseudomonas aeruginosa responds to exogenous polyunsaturated fatty acids (PUFAs) by modifying phospholipid composition, membrane permeability, and phenotypes associated with virulence. BMC Microbiol. 18 (1), 117.
- Beam, J.E., Wagner, N.J., Lu, K.Y., Parsons, J.B., Fowler Jr., V.G., Rowe, S.E., Conlon, B. P., 2023. Inflammasome-mediated glucose limitation induces antibiotic tolerance in Staphylococcus aureus. iScience 26 (10), 107942.
- Brouwers, H., Jónasdóttir, H.S., Kuipers, M.E., Kwekkeboom, J.C., Auger, J.L., Gonzalez-Torres, M., et al., 2020. Anti-inflammatory and proresolving effects of the omega-6 polyunsaturated fatty acid adrenic acid. J. Immunol. 205 (10), 2840–2849.
- Burgardt, A., Moustafa, A., Persicke, M., Sproß, J., Patschkowski, T., Risse, J.M., Peters-Wendisch, P., Lee, J.H., Wendisch, V.F., 2021. Coenzyme Q₁₀ biosynthesis established in the non-ubiquinone containing Corynebacterium glutamicum by metabolic engineering. Front. Bioeng. Biotechnol. 9, 650961.
- Calatayud, M., Dezutter, O., Hernandez-Sanabria, E., Hidalgo-Martinez, S., Meysman, F. J.R., Van de Wiele, T., 2019. Development of a host-microbiome model of the small intestine. FASEB J. 33 (3), 3985–3996.
- Devriese, S., Van den Bossche, L., Van Welden, S., Holvoet, T., Pinheiro, I., Hindryckx, P., De Vos, M., Laukens, D., 2017. T84 monolayers are superior to Caco-2 as a model system of colonocytes. Histochem. Cell Biol. 148 (1), 85–93.
- Didriksen, B.J., Eshleman, E.M., Alenghat, T., 2024. Epithelial regulation of microbiotaimmune cell dynamics. Mucosal Immunol. 17 (2), 303–313.
- Dissanayake, W.M.N., Chandanee, M.R., Lee, S.M., Heo, J.M., Yi, Y.J., 2023. Change in intestinal alkaline phosphatase activity is a hallmark of antibiotic-induced intestinal dysbiosis. Anim. Biosci. 36 (9), 1403–1413.
- Duche, R.T., Singh, A., Wandhare, A.G., Sangwan, V., Sihag, M.K., Nwagu, T.N.T., Panwar, H., Ezeogu, L.I., 2023. Antibiotic resistance in potential probiotic lactic acid bacteria of fermented foods and human origin from Nigeria. BMC Microbiol. 23 (1), 142
- Estaki, M., DeCoffe, D., Gibson, D.L., 2014. Interplay between intestinal alkaline phosphatase, diet, gut microbes and immunity. World J. Gastroenterol. 20 (42), 15650-15656
- Etienne-Mesmin, L., Vijay-Kumar, M., Gewirtz, A.T., Chassaing, B., 2016. Hepatocyte toll-like receptor 5 promotes bacterial clearance and protects mice against high-fat diet-induced liver disease. Cell Mol. Gastroenterol. Hepatol. 2 (5), 584–604.
- Fan, J., Xu, W., Xu, X., Wang, Y., 2022. Production of Coenzyme Q_{10} by microbes: an update. World J. Microbiol Biotechnol. 38 (11), 194.
- Felípez, L., Sentongo, T.A., 2009. Drug-induced nutrient deficiencies. Pediatr. Clin. North Am. 56 (5), 1211–1224.
- García-Mantrana, I., Monedero, V., Haros, M., 2025. Reduction of phytate in soy drink by fermentation with lactobacillus casei expressing phytases from bifidobacteria. Plant Foods Hum. Nutr. 70 (3), 269–274.
- Ghadimi, D., Fölster-Holst, R., Blömer, S., Ebsen, M., Röcken, C., Uchiyama, J., Shigenobu Matsuzaki, S., Bockelmann, W., 2024. Intricate crosstalk between food allergens, phages, bacteria, and eukaryotic host cells of the gut-skin axis. Yale J. Biol. Med. 97 (3), 309–324.
- Ghadimi, D., Fölster-Holst, R., Ebsen, M., Röcken, C., Dörfer, C., Uchiyama, J., Matsuzaki, S., W Bockelmann, W., 2023. Exploring The interplay between nutrients, bacteriophages, and bacterial lipases in host-and bacteria-mediated pathogenesis. Endocr. Metab. Immune Disord. Drug Targets 24 (8), 930–945.
- Goudarzi, F., Kiani, A., Nami, Y., Shahmohammadi, A., Mohammadalipour, A., Karami, A., Haghshenas, B., 2024. Potential probiotic Lactobacillus delbrueckii subsp. lactis KUMS-Y33 suppresses adipogenesis and promotes osteogenesis in human adipose-derived mesenchymal stem cell. Sci. Rep. 14 (1), 9689.
- Gross, J.L., Basu, R., Bradfield, C.J., Sun, J., John, S.P., Das, S., Dekker, J.P., Weiss, D.S., Fraser, I.D.C., 2024. Bactericidal antibiotic treatment induces damaging inflammation via TLR9. sensing of bacterial DNA. Nat. Commun. 15 (1), 10359.

Ham, S., Kim, H.-S., Jo, M.J., Cha, E., Ryoo, H.-S., Kim, H., Lee, H., Ko, G.-J., Park, H.-D., 2025. Synergistic treatment of linoleic acid and cefazolin on Staphylococcus aureus biofilm-related catheter infections. Appl. Environ. Microbiol. 91 (6), e0077025.

- Hsu, C.L., Schnabl, B., 2023. The gut-liver axis and gut microbiota in health and liver disease. Nat. Rev. Microbiol. 21 (11), 719–733.
- Hu, C., Xuan, Y., Zhang, X., Liu, Y., Yang, S., Yang, K., 2022. Immune cell metabolism and metabolic reprogramming. Mol. Biol. Rep. 49 (10), 9783–9795.
- Innes, J.K., Calder, P.C., 2018. Omega-6 fatty acids and inflammation. Prostaglandins Leukot. Ess. Fat. Acids 132, 41–48.
- Jung, J.W., Park, S.Y., Kim, H., 2022. Drug-induced vitamin deficiency. Ann. Clin. Nutr. Metab. 14 (1), 20–31.
- Kaviani, E., Hajibabaie, F., Abedpoor, N., Safavi, K., 2025. Synergic effects and possible mechanism of omega-6 fatty acids (ω-6) on immune system, inflammation, and cancer. Mol. Nutr. Food Res 69 (12), e70092.
- Klein, S.G., Serchi, T., Hoffmann, L., Blömeke, B., Gutleb, A.C., 2013. An improved 3D tetraculture system mimicking the cellular organisation at the alveolar barrier to study the potential toxic effects of particles on the lung. Part Fibre Toxicol. 10, 31.
- Lai, H.T.M., Ryder, N.A., Tintle, N.L., Jackson, K.H., Kris-Etherton, P.M., Harris, W.S., 2025. Red blood cell omega-6 fatty acids and biomarkers of inflammation in the framingham offspring study. Nutrients 17 (13), 2076.
- Lee, S.Q., Tan, T.S., Kawamukai, M., Chen, E.S., 2017. Cellular factories for coenzyme Q10 production. Microb Cell Fact. 16 (1), 39.
- Li, X., Gu, N., Huang, T.Y., Zhong, F., Peng, G., 2023. Pseudomonas aeruginosa: A typical biofilm forming pathogen and an emerging but underestimated pathogen in food processing. Front. Microbiol. 13, 1114199.
- Liu, T., Chamkha, I., Elmér, E., Sjövall, F., Ehinger, J.K., 2025. Antibiotic-induced mitochondrial dysfunction: Exploring tissue-specific effects on HEI-OC1 cells and peripheral blood mononuclear cells. Biochim. Biophys. Acta Gen. Subj. 1869 (9), 130832.
- Liu, Q., Yu, Z., Tian, F., Zhao, J., Zhang, H., Zhai, Q., Chen, W., 2020. Surface components and metabolites of probiotics for regulation of intestinal epithelial barrier. Microb. Cell Fact. 19 (1), 23.
- Liu, P., Zhang, Y., Zhang, Z., Huang, X., Su, X., Yang, S., Xie, Y., 2023. Antibiotic-Induced dysbiosis of the gut microbiota impairs gene expression in gut-liver axis of mice. Genes 14 (7), 1423.
- Llewellyn, A., Foey, A., 2017. Probiotic modulation of innate cell pathogen sensing and signaling events. Nutrients 9 (10), 1156.
- Luo, Y., Li, Y., Song, X., Wang, Y., Liu, S., Ren, F., Zhang, H., 2025. Enhanced solubility and bioavailability of coenzyme Q10 via co-amorphous system using stevioside. NPJ Sci. Food 9 (1), 98.
- Mantle, D., Golomb, B.A., 2025. Coenzyme Q10 and xenobiotic metabolism: an overview. Int. J. Mol. Sci. 26 (12), 5788.
- Marklund, M., Wu, J.H.Y., Imamura, F., Del Gobbo, L.C., Fretts, A., de Goede, J., et al., 2019. Biomarkers of dietary omega-6 fatty acids and incident cardiovascular disease and mortality. Circulation 139 (21), 2422–2436.
- Matthaiou, A.M., Tomos, I., Chaniotaki, S., Liakopoulos, D., Sakellaropoulou, K., Koukidou, S., Gheorghe, L.M., Eskioglou, S., Paspalli, A., Hillas, G., Dimakou, K., 2023. Association of broad-spectrum antibiotic therapy and vitamin e supplementation with vitamin K deficiency-induced coagulopathy: a case report and narrative review of the literature. J. Pers. Med 13 (9), 1349.
- Mohanty, D., Panda, S., Kumar, S., Ray, P., 2019. In vitro evaluation of adherence and anti-infective property of probiotic Lactobacillus plantarum DM 69 against Salmonella enterica. Microb. Pathog. 126, 212–217.
- Muller, P.A., Matheis, F., Mucida, D., 2020. Gut macrophages: key players in intestinal immunity and tissue physiology. Curr. Opin. Immunol. 62, 54–61.
- Murali, M., Alka, G., 2024. Could the microbial to host cell numbers in healthy multicellular organisms be following the golden ratio? Curr. Sci. 126 (8), 878–8812024.
- Murea, E.M., LaLonde, B.D., 2017. The effects of antibiotics on nutrient digestion. J. Emerg. Investig. 8 (1), 1–10. https://doi.org/10.59720/17-014.
- Nakagaki, B.N., Vieira, A.T., Rezende, R.M., David, B.A., Menezes, G.B., 2018. Tissue macrophages as mediators of a healthy relationship with gut commensal microbiota. Cell Immunol. 330, 16–26.
- Patangia, D.V., Anthony Ryan, C., Dempsey, E., Paul Ross, R., Stanton, C., 2022. Impact of antibiotics on the human microbiome and consequences for host health. MicrobiologyOpen 11 (1), e1260.
- Peng, M., Tabashsum, Z., Patel, P., Bernhardt, C., Biswas, D., 2018. Linoleic acids overproducing *Lactobacillus casei* limits growth, survival, and virulence of salmonella typhimurium and enterohaemorrhagic *Escherichia coli*. Front Microbiol 9, 2663.
- Perdijk, O., Butler, A., Macowan, M., Chatzis, R., Bulanda, E., Grant, R.D., Harris, N.L., Wypych, T.P., Marsland, B.J., 2024. Antibiotic-driven dysbiosis in early life disrupts indole-3-propionic acid production and exacerbates allergic airway inflammation in adulthood. Immunity 57 (8), 1939–1954 e7.
- Poli, A., Agostoni, C., Visioli, F., 2023. Dietary fatty acids and inflammation: focus on the n-6 series. Int J. Mol. Sci. 24 (5), 4567.
- Ramsay, K.A., Rehman, A., Wardell, S.T., Martin, L.W., Bell, S.C., Patrick, W.M., Winstanley, C., Lamont, I.L., 2023. Ceftazidime resistance in Pseudomonas aeruginosa is multigenic and complex. PLOS One 18 (5), e0285856.
- Rehman, K., Aluwi, M.F., Rullah, K., Wai, L.K., Mohd Amin, M.C., Zulfakar, M.H., 2015. Probing the effects of fish oil on the delivery and inflammation-inducing potential of imiquimod. Int J. Pharm. 490 (1-2), 131–141.
- Ren, C., Cheng, L., Sun, Y., Zhang, Q., de Haan, B.J., Zhang, H., Faas, M.M., de Vos, Paul, 2020. Lactic acid bacteria secrete toll like receptor 2 stimulating and macrophage immunomodulating bioactive factors. J. Funct. Foods 66, 103783.
- Saini, R.K., Keum, Y.S., 2018. Omega-3 and omega-6 polyunsaturated fatty acids: Dietary sources, metabolism, and significance - a review. Life Sci. 203, 255–267.

Schulze, R.J., Schott, M.B., Casey, C.A., Tuma, P.L., McNiven, M.A., 2019. The cell biology of the hepatocyte: a membrane trafficking machine. J. Cell Biol. 218 (7), 2096–2112

- Sender, R., Fuchs, S., Milo, R., 2016. Are we really vastly outnumbered? Revisiting the ratio of bacterial to host cells in humans. Cell 164 (3), 337–340.
- Shobha, 2019. Antibiotics and nutritional implications- the drugs-nutrients interactions. Acta Sci. Nutr. Health 3 (6), 51–54.
- Sifuentes-Franco, S., Sánchez-Macías, D.C., Carrillo-Ibarra, S., Rivera-Valdés, J.J., Zuñiga, L.Y., Sánchez-López, V.A., 2022. Antioxidant and anti-inflammatory effects of coenzyme Q10 supplementation on infectious diseases. Healthcare 10 (3), 487.
- Taitz, J.J., Tan, J., Ni, D., Potier-Villette, C., Grau, G., Nanan, R., Macia, L., 2025.
 Antibiotic-mediated dysbiosis leads to activation of inflammatory pathways. Front.
 Immunol. 15, 1493991.
- Tang, J., Wang, X., Chen, S., Chang, T., Gu, Y., Zhang, F., Hou, J., Luo, Y., Li, M., Huang, J., Liu, M., Zhang, L., Wang, Y., Shen, X., Xu, L., 2024. Disruption of glucose homeostasis by bacterial infection orchestrates host innate immunity through NAD ⁺/NADH balance. Cell Rep. 43 (9), 114648.
- Tang, Y., Yu, C., Rao, L., 2024. Engineering bacteria and their derivatives for cancer immunotherapy. BME Front. 5, 0047.
- Tou, K.A.S., Rehman, K., Ishak, W.M.W., Zulfakar, M.H., 2019. Influence of omega fatty acids on skin permeation of a coenzyme Q10 nanoemulsion cream formulation: characterization, in silico and ex vivo determination. Drug Dev. Ind. Pharm. 45 (9), 1451–1458.
- Traven, A., Naderer, T., 2019. Central metabolic interactions of immune cells and microbes: prospects for defeating infections. EMBO Rep. 20 (7), e47995.
- Troha, K., Ayres, J.S., 2020. Metabolic adaptations to infections at the organismal level. Trends Immunol. 41 (2), 113–125.
- Uchiyama, J., Suzuki, M., Nishifuji, K., Kato, S.I., Miyata, R., Nasukawa, T., Yamaguchi, K., Takemura-Uchiyama, I., Ujihara, T., Shimakura, H., Murakami, H., Okamoto, N., Sakaguchi, Y., Shibayama, K., Sakaguchi, M., Matsuzaki, S., 2016. Analyses of short-term antagonistic evolution of pseudomonas aeruginosa strain

- PAO1 and phage KPP22 (Myoviridae Family, PB1-Like Virus Genus). Appl. Environ. Microbiol. 82 (15), 4482–4491.
- Vebr, M., Pomahačová, R., Sýkora, J., Schwarz, J., 2023. A narrative review of cytokine networks: pathophysiological and therapeutic implications for inflammatory bowel disease pathogenesis. Biomedicines 11 (12), 3229.
- Vliex, L.M.M., Penders, J., Nauta, A., Zoetendal, E.G., Blaak, E.E., 2024. The individual response to antibiotics and diet - insights into gut microbial resilience and host metabolism. Nat. Rev. Endocrinol. 20 (7), 387–398.
- Wood, S.J., Goldufsky, J.W., Seu, M.Y., Dorafshar, A.H., Shafikhani, S.H., 2023.Pseudomonas aeruginosa cytotoxins: mechanisms of cytotoxicity and impact on inflammatory responses. Cells 12 (1), 195.
- Xu, R., Molenaar, A.J., Chen, Z., Yuan, Y., 2025. Mode and mechanism of action of omega-3 and omega-6 unsaturated fatty acids in chronic diseases. Nutrients 17 (9), 1540.
- Yang, J.H., Bhargava, P., McCloskey, D., Mao, N., Palsson, B.O., Collins, J.J., 2017.
 Antibiotic-induced changes to the host metabolic environment inhibit drug efficacy and alter immune function. Cell Host Microbe 22 (6), 757–765 e3.
- Yang, B., Zhou, Y., Wu, M., Li, X., Mai, K., Ai, Q., 2020. @-6 Polyunsaturated fatty acids (linoleic acid) activate both autophagy and antioxidation in a synergistic feedback loop via TOR-dependent and TOR-independent signaling pathways. Cell Death Dis. 11 (7), 607.
- Yip, A.Y.G., King, O.G., Omelchenko, O., Kurkimat, S., Horrocks, V., Mostyn, P., Danckert, N., Ghani, R., Satta, G., Jauneikaite, E., Davies, F.J., Clarke, T.B., Mullish, B.H., Marchesi, J.R., McDonald, J.A.K., 2023. Antibiotics promote intestinal growth of carbapenem-resistant Enterobacteriaceae by enriching nutrients and depleting microbial metabolites. Nat. Commun. 14 (1), 5094.
- Zou, J., Tian, Z., Zhao, Y., Qiu, X., Mao, Y., Li, K., Shi, Y., Zhao, D., Liang, Y., Ji, Q., Ling, W., Yang, Y., 2022. Coenzyme Q10 supplementation improves cholesterol efflux capacity and antiinflammatory properties of high-density lipoprotein in Chinese adults with dyslipidemia. Nutrition 101, 111703.